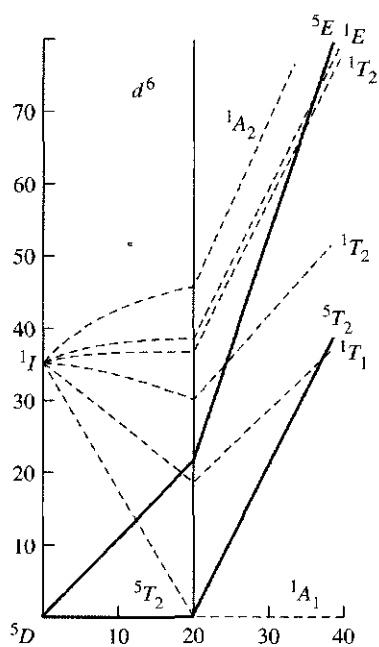


## CHAPTER

## 11

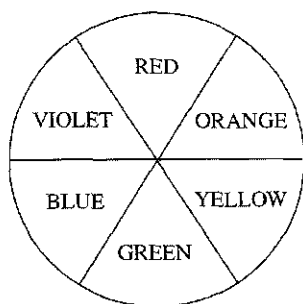
Coordination  
Chemistry III:  
Electronic Spectra

Perhaps the most striking aspect of many coordination compounds of transition metals is that they have vivid colors. The dye Prussian blue, for example, has been used as a pigment for more than two centuries (and is still used in blueprints); it is a complicated coordination compound involving iron(II) and iron(III) coordinated octahedrally by cyanide. Many precious gems exhibit colors resulting from transition metal ions incorporated into their crystalline lattices. For example, emeralds are green as a consequence of the incorporation of small amounts of chromium(III) into crystalline  $\text{Be}_3\text{Al}_2\text{Si}_6\text{O}_{18}$ ; amethysts are violet as a result of the presence of small amounts of iron(II), iron(III), and titanium(IV) in an  $\text{Al}_2\text{O}_3$  lattice; and rubies are red because of chromium(III), also in a lattice of  $\text{Al}_2\text{O}_3$ . The color of blood is caused by the red heme group, a coordination compound of iron present in hemoglobin. Most readers are probably familiar with blue  $\text{CuSO}_4 \cdot 5\text{H}_2\text{O}$ , a compound often used to demonstrate the growing of large, highly symmetric crystals.

It is desirable to understand why so many coordination compounds are colored, in contrast to most organic compounds, which are transparent, or nearly so, in the visible spectrum. We will first review the concept of light absorption and how it is measured. The ultraviolet and visible spectra of coordination compounds of transition metals involve transitions between the  $d$  orbitals of the metals. Therefore, we will need to look closely at the energies of these orbitals (as discussed in Chapter 10) and at the possible ways in which electrons can be raised from lower to higher energy levels. The energy levels of  $d$  electron configurations (as opposed to the energies of *individual* electrons) are somewhat more complicated than might be expected, and we need to consider how electrons in atomic orbitals can interact with each other.

For many coordination compounds, the electronic absorption spectrum provides a convenient method for determining the magnitude of the effect of ligands on the  $d$  orbitals of the metal. Although in principle we can study this effect for coordination compounds of any geometry, we will concentrate on the most common geometry, octahedral, and will examine how the absorption spectrum can be used to determine the magnitude of the octahedral ligand field parameter  $\Delta_o$  for a variety of complexes.

## 11-1 ABSORPTION OF LIGHT



In explaining the colors of coordination compounds, we are dealing with the phenomenon of *complementary colors*: if a compound absorbs light of one color, we see the complement of that color. For example, when white light (containing a broad spectrum of all visible wavelengths) passes through a substance that absorbs red light, the color observed is green. Green is the complement of red, so green predominates visually when red light is subtracted from white. Complementary colors can conveniently be remembered as the color pairs on opposite sides of the color wheel shown in the margin.

An example from coordination chemistry is the deep blue color of aqueous solutions of copper(II) compounds, containing the ion  $[\text{Cu}(\text{H}_2\text{O})_6]^{2+}$ . The blue color is a consequence of the absorption of light between approximately 600 and 1000 nm (maximum near 800 nm; Figure 11-1), in the yellow to infrared region of the spectrum. The color observed, blue, is the average complementary color of the light absorbed.

It is not always possible to make a simple prediction of color directly from the absorption spectrum, in large part because many coordination compounds contain two or more absorption bands of different energies and intensities. The net color observed is the color predominating after the various absorptions are removed from white light.

For reference, the approximate wavelengths and complementary colors to the principal colors of the visible spectrum are given in Table 11-1.

### 11-1-1 BEER-LAMBERT ABSORPTION LAW

If light of intensity  $I_0$  at a given wavelength passes through a solution containing a species that absorbs light, the light emerges with intensity  $I$ , which may be measured by a suitable detector (Figure 11-2).

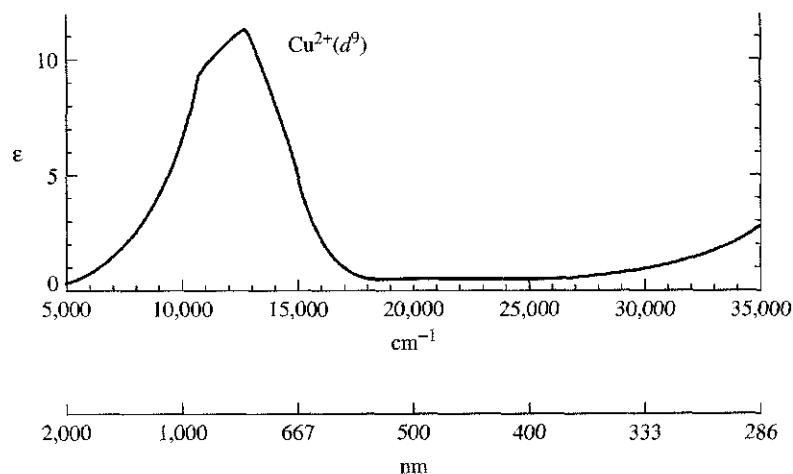


**FIGURE 11-1** Absorption Spectrum of  $[\text{Cu}(\text{H}_2\text{O})_6]^{2+}$ . (Reproduced with permission from B. N. Figgis, *Introduction to Ligand Fields*, Wiley-Interscience, New York, 1966, p. 221.)

**TABLE 11-1**  
Visible Light and Complementary Colors

Wavelength Range (nm)	Wave Numbers ( $\text{cm}^{-1}$ )	Color	Complementary Color
<400	>25,000	Ultraviolet	
400–450	22,000–25,000	Violet	Yellow
450–490	20,000–22,000	Blue	Orange
490–550	18,000–20,000	Green	Red
550–580	17,000–18,000	Yellow	Violet
580–650	15,000–17,000	Orange	Blue
650–700	14,000–15,000	Red	Green
>700	<14,000	Infrared	

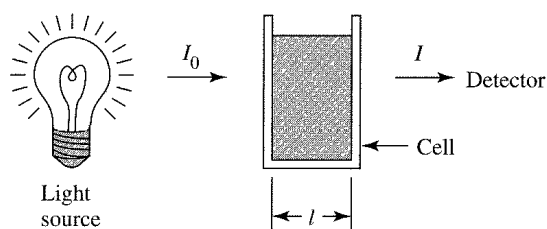


**FIGURE 11-2** Absorption of Light by Solution.

The Beer-Lambert law may be used to describe the absorption of light (ignoring scattering and reflection of light from cell surfaces) at a given wavelength by an absorbing species in solution:

$$\log \frac{I_0}{I} = A = \epsilon lc$$

where  $A$  = absorbance

$\epsilon$  = molar absorptivity ( $\text{L mol}^{-1} \text{cm}^{-1}$ ) (also known as molar extinction coefficient)

$l$  = path length through solution (cm)

$c$  = concentration of absorbing species ( $\text{mol L}^{-1}$ )

Absorbance is a dimensionless quantity. An absorbance of 1.0 corresponds to 90% absorption at a given wavelength,<sup>1</sup> an absorbance of 2.0 corresponds to 99% absorption, and so on. The most common units of the other quantities in the Beer-Lambert law are shown in parentheses above.

Spectrophotometers commonly obtain spectra as plots of absorbance versus wavelength. The molar absorptivity is a characteristic of the species that is absorbing the light and is highly dependent on wavelength. A plot of molar absorptivity versus wavelength gives a spectrum characteristic of the molecule or ion in question, as in Figure 11-1. As we will see, this spectrum is a consequence of transitions between states of different energies and can provide valuable information about those states and, in turn, about the structure and bonding of the molecule or ion.

Although the quantity most commonly used to describe absorbed light is the wavelength, energy and frequency are also used. In addition, the wavenumber (the number of waves per centimeter), a quantity proportional to the energy, is frequently used, especially in reference to infrared light. For reference, the relations between these quantities are given by the equations

$$E = h\nu = \frac{hc}{\lambda} = hc\left(\frac{1}{\lambda}\right) = hc\bar{\nu}$$

where  $E$  = energy

$h$  = Planck's constant =  $6.626 \times 10^{-34} \text{ J s}$

$c$  = speed of light =  $2.998 \times 10^8 \text{ m s}^{-1}$

$\nu$  = frequency ( $\text{s}^{-1}$ )

$\lambda$  = wavelength (often reported in nm)

$\frac{1}{\lambda} = \bar{\nu}$  = wavenumber ( $\text{cm}^{-1}$ )

<sup>1</sup>For absorbance = 1.0,  $\log(I_0/I) = 1.0$ . Therefore,  $I_0/I = 10$ , and  $I = 0.10 I_0 = 10\% \times I_0$ ; 10% of the light is transmitted, and 90% is absorbed.

## 11-2 QUANTUM NUMBERS OF MULTIELECTRON ATOMS

Absorption of light results in the excitation of electrons from lower to higher energy states; because such states are quantized, we observe absorption in "bands" (as in Figure 11-1), with the energy of each band corresponding to the difference in energy between the initial and final states. To gain insight into these states and the energy transitions between them, we first need to consider how electrons in atoms can interact with each other.

Although the quantum numbers and energies of individual electrons can be described in fairly simple terms, interactions between electrons complicate this picture. Some of these interactions were discussed in Section 2-2-3: as a result of repulsions between electrons (characterized by energy  $\Pi_c$ ), electrons tend to occupy separate orbitals; as a result of exchange energy ( $\Pi_e$ ), electrons in separate orbitals tend to have parallel spins.

Consider again the example of the energy levels of a carbon atom. Carbon has the electron configuration  $1s^2 2s^2 2p^2$ . At first glance, we might expect the  $p$  electrons to have the same energy. However, there are three major energy levels for the  $p^2$  electrons differing in energy by pairing and exchange energies ( $\Pi_c$  and  $\Pi_e$ ) and, in addition, the lowest major energy level is split into three slightly different energies, for a total of five energy levels. As an alternative to the discussion presented in Section 2-2-3, each energy level can be described as a combination of the  $m_l$  and  $m_s$  values of the  $2p$  electrons.

*Independently*, each of the  $2p$  electrons could have any of six possible  $m_l, m_s$  combinations:

$$\begin{array}{ll} n = 2, l = 1 & \text{(quantum numbers defining } 2p \text{ orbitals)} \\ m_l = +1, 0, \text{ or } -1 & \text{(three possible values)} \\ m_s = +\frac{1}{2} \text{ or } -\frac{1}{2} & \text{(two possible values)} \end{array}$$

The  $2p$  electrons are not independent of each other, however; the orbital angular momenta (characterized by  $m_l$  values) and the spin angular momenta (characterized by  $m_s$  values) of the  $2p$  electrons interact in a manner called **Russell-Saunders coupling** or **LS coupling**.<sup>2</sup> The interactions produce atomic states called **microstates** that can be described by new quantum numbers:

$$\begin{array}{ll} M_L = \sum m_l & \text{Total orbital angular momentum} \\ M_S = \sum m_s & \text{Total spin angular momentum} \end{array}$$

We need to determine how many possible combinations of  $m_l$  and  $m_s$  values there are for a  $p^2$  configuration.<sup>3</sup> Once these combinations are known, we can determine the corresponding values of  $M_L$  and  $M_S$ . For shorthand, we will designate the  $m_s$  value of each electron by a superscript  $+$ , representing  $m_s = +\frac{1}{2}$ , or  $-$ , representing  $m_s = -\frac{1}{2}$ . For example, an electron having  $m_l = +1$  and  $m_s = +\frac{1}{2}$  will be written as  $1^+$ .

One possible set of values for the two electrons in the  $p^2$  configuration would be

$$\left. \begin{array}{l} \text{First electron: } m_l = +1 \text{ and } m_s = +\frac{1}{2} \\ \text{Second electron: } m_l = 0 \text{ and } m_s = -\frac{1}{2} \end{array} \right\} \text{Notation: } 1^+0^-$$

Each set of possible quantum numbers (such as  $1^+0^-$ ) is called a microstate.

<sup>2</sup>For a more advanced discussion of coupling and its underlying theory, see M. Gerloch, *Orbitals, Terms, and States*, Wiley-Interscience, New York, 1986.

<sup>3</sup>Electrons in filled orbitals can be ignored, because their net spin and angular momenta are both zero.

The next step is to tabulate the possible microstates. In doing this, we need to take two precautions: (1) to be sure that no two electrons in the same microstate have identical quantum numbers (the Pauli exclusion principle applies); and (2) to count only the *unique* microstates. For example, the microstates  $1^+0^-$  and  $0^-1^+$ ,  $0^+0^-$  and  $0^-0^+$  in a  $p^2$  configuration are duplicates and only one of each pair will be listed.

If we determine all possible microstates and tabulate them according to their  $M_L$  and  $M_S$  values, we obtain a total of 15 microstates.<sup>4</sup> These microstates can be arranged according to their  $M_L$  and  $M_S$  values and listed conveniently in a microstate table, as shown in Table 11-2.

TABLE 11-2  
Microstate Table for  $p^2$

		$M_S$		
		-1	0	+1
$M_L$	+2		$1^+ 1^-$	
	+1	$1^- 0^-$	$1^+ 0^-$ $1^- 0^+$	$1^+ 0^+$
	0	$-1^- 1^-$	$-1^+ 1^-$ $0^+ 0^-$ $-1^- 1^+$	$-1^+ 1^+$
	-1	$-1^- 0^-$	$-1^+ 0^-$ $-1^- 0^+$	$-1^+ 0^+$
	-2		$-1^+ -1^-$	

#### EXAMPLE

Determine the possible microstates for an  $s^1p^1$  configuration and use them to prepare a microstate table.

The  $s$  electron can have  $m_l = 0$  and  $m_s = \pm \frac{1}{2}$ .

The  $p$  electron can have  $m_l = +1, 0, -1$  and  $m_s = \pm \frac{1}{2}$ .

The resulting microstate table is then

		$M_S$		
		-1	0	+1
$M_L$	+1	$0^- 1^-$	$0^- 1^+$ $0^+ 1^-$	$0^+ 1^+$
	0	$0^- 0^-$	$0^+ 0^-$ $0^- 0^+$	$0^+ 0^+$
	-1	$0^- -1^-$	$0^- -1^+$ $0^+ -1^-$	$0^+ -1^+$

<sup>4</sup>The number of microstates =  $i!/j!(i-j)!$ , where  $i$  = number of  $m_l, m_s$  combinations (six here, because  $m_l$  can have values of 1, 0, and -1 and  $m_s$  can have values of  $+\frac{1}{2}$  and  $-\frac{1}{2}$ ) and  $j$  = number of electrons.

In this case,  $0^+0^-$  and  $0^-0^+$  are different microstates, because the first electron is an  $s$  and the second electron is a  $p$ ; both must be counted.

### EXERCISE 11-1

Determine the possible microstates for a  $d^2$  configuration and use them to prepare a microstate table. (Your table should contain 45 microstates.)

We have now seen how electronic quantum numbers  $m_l$  and  $m_s$  may be combined into atomic quantum numbers  $M_L$  and  $M_S$ , which describe atomic microstates.  $M_L$  and  $M_S$ , in turn, give atomic quantum numbers  $L$ ,  $S$ , and  $J$ . These quantum numbers collectively describe the energy and symmetry of an atom or ion and determine the possible transitions between states of different energies. These transitions account for the colors observed for many coordination complexes, as will be discussed later in this chapter.

The quantum numbers that describe states of multielectron atoms are defined as follows:

$L$  = total orbital angular momentum quantum number

$S$  = total spin angular momentum quantum number

$J$  = total angular momentum quantum number

These total angular momentum quantum numbers are determined by vector sums of the individual quantum numbers; determination of their values is described in this section and the next.

Quantum numbers  $L$  and  $S$  describe collections of microstates, whereas  $M_L$  and  $M_S$  describe the microstates themselves.  $L$  and  $S$  are the largest possible values of  $M_L$  and  $M_S$ .  $M_L$  is related to  $L$  much as  $m_l$  is related to  $l$ , and the values of  $M_S$  and  $m_s$  are similarly related:

Atomic States	Individual Electrons
$M_L = 0, \pm 1, \pm 2, \dots, \pm L$	$m_l = 0, \pm 1, \pm 2, \dots, \pm l$
$M_S = S, S - 1, S - 2, \dots, -S$	$m_s = +\frac{1}{2}, -\frac{1}{2}$

Just as the quantum number  $m_l$  describes the component of the quantum number  $l$  in the direction of a magnetic field for an electron, the quantum number  $M_L$  describes the component of  $L$  in the direction of a magnetic field for an atomic state. Similarly,  $m_s$  describes the component of an electron's spin in a reference direction, and  $M_S$  describes the component of  $S$  in a reference direction for an atomic state.

The values of  $L$  correspond to atomic states described as  $S$ ,  $P$ ,  $D$ ,  $F$ , and higher states in a manner similar to the designation of atomic orbitals as  $s$ ,  $p$ ,  $d$ , and  $f$ . The values of  $S$  are used to calculate the **spin multiplicity**, defined as  $2S + 1$ . For example, states having spin multiplicities of 1, 2, 3, and 4, are described as singlet, doublet, triplet, and quartet states. The spin multiplicity is designated as a left superscript. Examples of atomic states are given in Table 11-3 and in the examples that follow.<sup>5</sup>

Atomic states characterized by  $S$  and  $L$  are often called **free-ion terms** (sometimes Russell-Saunders terms) because they describe individual atoms or ions, free of ligands.

$L = 0$	$S$ state
$L = 1$	$P$ state
$L = 2$	$D$ state
$L = 3$	$F$ state

<sup>5</sup>Unfortunately,  $S$  is used in two ways: to designate the atomic spin quantum number and to designate a state having  $L = 0$ . Chemists are not always wise in choosing their symbols!

**TABLE 11-3**  
Examples of Atomic States (Free-ion Terms) and Quantum Numbers

Term	$L$	$S$
$^1S$	0	0
$^2S$	0	$\frac{1}{2}$
$^3P$	1	1
$^4D$	2	$\frac{3}{2}$
$^5F$	3	2

Their labels are often called **term symbols**.<sup>6</sup> Term symbols are composed of a letter relating to the value of  $L$  and a left superscript for the spin multiplicity. For example, the term symbol  $^3D$  corresponds to a state in which  $L = 2$  and the spin multiplicity ( $2S + 1$ ) is 3;  $^5F$  marks a state in which  $L = 3$  and  $2S + 1 = 5$ .

Free-ion terms are very important in the interpretation of the spectra of coordination compounds. The following examples show how to determine the values of  $L$ ,  $M_L$ ,  $S$ , and  $M_S$  for a given term and how to prepare microstate tables from them.

### EXAMPLES

**$^1S$  (singlet  $S$ )** An  $S$  term has  $L = 0$  and must therefore have  $M_L = 0$ . The spin multiplicity (the superscript) is  $2S + 1$ . Because  $2S + 1 = 1$ ,  $S$  must equal 0 (and  $M_S = 0$ ). There can be only one microstate, having  $M_L = 0$  and  $M_S = 0$  for a  $^1S$  term. For the minimum configuration of two electrons:

		$M_S$					
			0				$M_S$
	$M_L$	0	0 <sup>+</sup> 0 <sup>-</sup>	or	$M_L$	0	x

Each microstate is designated by  $x$  in the second form of the table.

**$^2P$  (doublet  $P$ )** A  $P$  term has  $L = 1$ ; therefore,  $M_L$  can have three values: +1, 0, and -1. The spin multiplicity is  $2 = 2S + 1$ . Therefore,  $S = \frac{1}{2}$ , and  $M_S$  can have two values:  $+\frac{1}{2}$  and  $-\frac{1}{2}$ . There are six microstates in a  $^2P$  term (3 rows  $\times$  2 columns). For the minimum case of one electron:

			$M_S$					
			$-\frac{1}{2}$	$+\frac{1}{2}$			$M_S$	
		1	1 <sup>-</sup>	1 <sup>+</sup>		1	x	x
	$M_L$	0	0 <sup>-</sup>	0 <sup>+</sup>	or	$M_L$	0	x
		-1	-1 <sup>-</sup>	-1 <sup>+</sup>		-1	x	x

The spin multiplicity is equal to the number of possible values of  $M_S$ ; therefore, the spin multiplicity is simply the number of columns in the microstate table.

### EXERCISE 11-2

For each of the following free-ion terms, determine the values of  $L$ ,  $M_L$ ,  $S$ , and  $M_S$ , and diagram the microstate table as in the preceding examples:  $^2D$ ,  $^1P$ , and  $^2S$ .

At last, we are in a position to return to the  $p^2$  microstate table and reduce it to its constituent atomic states (terms). To do this, it is sufficient to designate each microstate simply by  $x$ ; it is important to tabulate the number of microstates, but it is not necessary to write out each microstate in full.

To reduce this microstate table into its component free-ion terms, note that each of the terms described in the examples and Exercise 11-2 consists of a rectangular array of microstates. To reduce the  $p^2$  microstate table into its terms, all that is necessary is to find the rectangular arrays. This process is illustrated in Table 11-4. Note that for each

<sup>6</sup>Although "term" and "state" are often used interchangeably, "term" is suggested as the preferred label for the results of Russell-Saunders coupling just described, and "state" for the results of spin-orbit coupling (described in the following section), including the quantum number  $J$ . In most cases, the meaning of "term" and "state" can be deduced from the context. See B. N. Figgis, "Ligand Field Theory," in G. Wilkinson, R. D. Gillard, and J. A. McCleverty, eds. *Comprehensive Coordination Chemistry*, Vol. 1, Pergamon Press, Elmsford, NY, 1987, p. 231.

term, the spin multiplicity is the same as the number of columns of microstates: a singlet term (such as  $^1D$ ) has a single column, a doublet term has two columns, a triplet term (such as  $^3P$ ) has three columns, and so forth.

Therefore, the  $p^2$  electron configuration gives rise to three free-ion terms, designated  $^3P$ ,  $^1D$ , and  $^1S$ . These terms have different energies; they represent three states with different degrees of electron-electron interactions. For our example of a  $p^2$  configuration for a carbon atom, the  $^3P$ ,  $^1D$ , and  $^1S$  terms have three distinct energies, the three major energy levels observed experimentally.

The final step in this procedure is to determine which term has the lowest energy. This can be done by using two of **Hund's rules**:

1. The ground term (term of lowest energy) has the highest spin multiplicity. In our example of  $p^2$ , therefore, the ground term is the  $^3P$ . This term can be identified as having the following configuration:



This is sometimes called Hund's rule of maximum multiplicity, introduced in Section 2-2-3.

2. If two or more terms share the maximum spin multiplicity, the ground term is the one having the highest value of  $L$ . For example, if  $^4P$  and  $^4F$  terms are both found for an electron configuration, the  $^4F$  has lower energy ( $^4F$  has  $L = 3$ ;  $^4P$  has  $L = 1$ ).

### EXAMPLE

Reduce the microstate table for the  $s^1p^1$  configuration to its component free-ion terms, and identify the ground-state term.

The microstate table (prepared in the example preceding Exercise 11-1) is the sum of the microstate tables for the  $^3P$  and  $^1P$  terms:

		$M_S$		
		-1	0	+1
$M_L$	+1	x	x	x
	0	x	x	x
	-1	x	x	x
		$^3P$		

		$M_S$		
		-1	0	+1
$M_L$	+1		x	
	0		x	
	-1		x	
		$^1P$		

Hund's rule of maximum multiplicity requires  $^3P$  as the ground state.

### EXERCISE 11-3

In Exercise 11-1, you obtained a microstate table for the  $d^2$  configuration. Reduce this to its component free-ion terms, and identify the ground-state term.



**TABLE 11-4**  
**The Microstate Table for  $p^2$  and its Reduction to Free-ion Terms**

		$M_S$		
		-1	0	+1
$M_L$	+2			
	+1	x	x	x
	0	x	x	x
	-1	x	x	x
	-2			

		$M_S$		
		-1	0	+1
$M_L$	+2		x	
	+1		x	
	0		x	
	-1		x	
	-2		x	

${}^1D$

		$M_S$		
		-1	0	+1
$M_L$	+2			
	+1	x	x	x
	0	x	x	x
	-1	x	x	x
	-2			

${}^3P$

		$M_S$		
		-1	0	+1
$M_L$	+2			
	+1			
	0		x	
	-1			
	-2			

${}^1S$

NOTE: The  ${}^1S$  and  ${}^1D$  terms have higher energy than the  ${}^3P$ , but cannot be identified with a single electron configuration. The relative energies of higher-energy terms like these also cannot be determined by simple rules.

### 11-2-1 SPIN-ORBIT COUPLING

To this point in the discussion of multielectron atoms, the spin and orbital angular momenta have been treated separately. In addition, the spin and orbital angular momenta couple with each other, a phenomenon known as spin-orbit coupling. In multielectron atoms, the  $S$  and  $L$  quantum numbers combine into the total angular momentum quantum number  $J$ . The quantum number  $J$  may have the following values:

$$J = L + S, L + S - 1, L + S - 2, \dots, |L - S|$$

The value of  $J$  is given as a subscript.

#### EXAMPLE

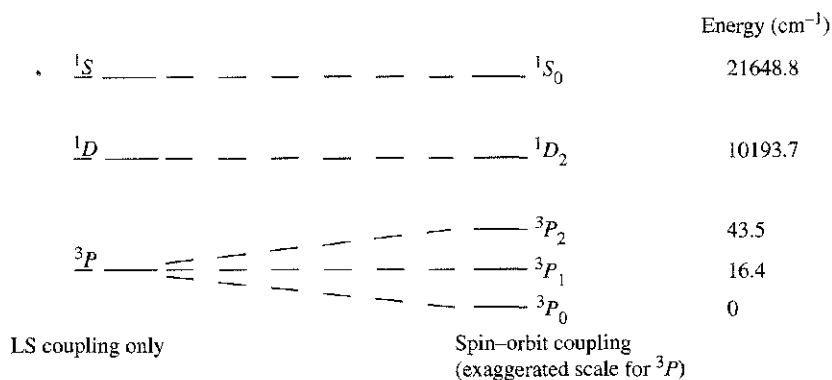
Determine the possible values of  $J$  for the carbon terms.

For the term symbols just described for carbon, the  ${}^1D$  and  ${}^1S$  terms each have only one  $J$  value, whereas the  ${}^3P$  term has three slightly different energies, each described by a different  $J$ .  $J$  can have only the value 0 for the  ${}^1S$  term ( $0 + 0$ ) and only the value 2 for the  ${}^1D$  term ( $2 + 0$ ). For the  ${}^3P$  term,  $J$  can have the three values 2, 1, and 0 ( $1 + 1$ ,  $1 + 1 - 1$ ,  $1 + 1 - 2$ ).

#### EXERCISE 11-4

Determine the possible values of  $J$  for the terms obtained from a  $d^2$  configuration in Exercise 11-3.

Spin-orbit coupling acts to split free-ion terms into states of different energies. The  $^3P$  term therefore splits into states of three different energies, and the total energy level diagram for the carbon atom can be shown as



These are the five energy states for the carbon atom referred to at the beginning of this section. The state of lowest energy (spin-orbit coupling included) can be predicted from **Hund's third rule**:

3. For subshells (such as  $p^2$ ) that are less than half-filled, the state having the lowest  $J$  value has the lowest energy ( $^3P_0$  above); for subshells that are more than half-filled, the state having the highest  $J$  value has the lowest energy. Half-filled subshells have only one possible  $J$  value.

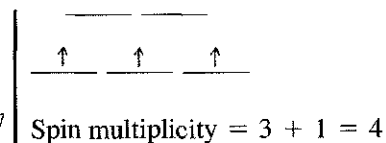
Spin-orbit coupling can have significant effects on the electronic spectra of coordination compounds, especially those involving fairly heavy metals (atomic number  $>40$ ).

### 11-3 ELECTRONIC SPECTRA OF COORDINATION COMPOUNDS

We can now make the connection between electron-electron interactions and the absorption spectra of coordination compounds. In Section 11-2, we considered a method for determining the microstates and free-ion terms for electron configurations. For example, a  $d^2$  configuration gives rise to five free-ion terms,  $^3F$ ,  $^3P$ ,  $^1G$ ,  $^1D$ , and  $^1S$ , with the  $^3F$  term of lowest energy (Exercises 11-1 and 11-3). Absorption spectra of coordination compounds in most cases involve the  $d$  orbitals of the metal, and it is consequently important to know the free-ion terms for the possible  $d$  configurations. Determining the microstates and free-ion terms for configurations of three or more electrons can be a tedious process. For reference, therefore, these are listed for the possible  $d$  electron configurations in Table 11-5.

In the interpretation of spectra of coordination compounds, it is often important to identify the lowest-energy term. A quick and fairly simple way to do this is given here, using as an example a  $d^3$  configuration in octahedral symmetry.

1. Sketch the energy levels, showing the  $d$  electrons.
2. Spin multiplicity of lowest-energy state = number of unpaired electrons + 1.<sup>7</sup>



<sup>7</sup>This is equivalent to the spin multiplicity =  $2S + 1$ , as shown previously.

**TABLE 11-5**  
**Free-ion Terms for  $d^n$  Configurations**

Configuration	Free-ion Terms
$d^1$	$^2D$
$d^2$	$^1S$ $^1D$ $^1G$ $^3P$ $^3F$
$d^3$	$^2D$ $^4P$ $^4F$ $^2P$ $^2D$ $^2F$ $^2G$ $^2H$
$d^4$	$^5D$ $^1S$ $^1D$ $^1G$ $^3P$ $^3F$ $^3P$ $^3D$ $^3F$ $^3G$ $^3H$ $^1S$ $^1D$ $^1F$ $^1G$ $^1I$
$d^5$	$^2D$ $^4P$ $^4F$ $^2P$ $^2D$ $^2F$ $^2G$ $^2H$ $^2S$ $^2D$ $^2F$ $^2G$ $^2I$ $^4D$ $^4G$ $^6S$
$d^6$	Same as $d^4$
$d^7$	Same as $d^3$
$d^8$	Same as $d^2$
$d^9$	Same as $d^1$
$d^{10}$	$^1S$

NOTE: For any configuration, the free-ion terms are the sum of those listed; for example, for the  $d^2$  configuration, the free-ion terms are  $^1S + ^1D + ^1G + ^3P + ^3F$ .

- Determine the maximum possible value of  $M_L$  (=sum of  $m_l$  values) for the configuration as shown. This determines the type of free-ion term (e.g.,  $S$ ,  $P$ ,  $D$ )
  - Combine results of Steps 2 and 3 to get the ground term:
- maximum possible value of  $m_l$  for three electrons as shown:  
 $2 + 1 + 0 = 3$   
 therefore,  $F$  term  
 $^4F$

Step 3 deserves elaboration. The maximum value of  $m_l$  for the first electron would be 2 (the highest value possible for a  $d$  electron). Because the electron spins are parallel, the second electron cannot also have  $m_l = 2$  (it would violate the exclusion principle); the highest value it can have is  $m_l = 1$ . Finally, the third electron cannot have  $m_l = 2$  or 1, because it would then have the same quantum numbers as one of the first two electrons; the highest  $m_l$  value this electron could have would therefore be 0. Consequently, the maximum value of  $M_L = 2 + 1 + 0 = 3$ .

#### EXAMPLE

$d^4$  (low spin):



2. Spin multiplicity =  $2 + 1 = 3$

3. Highest possible value of  $M_L = 2 + 2 + 1 + 0 = 5$ ; therefore,  $H$  term.

Note that here  $m_l = 2$  for the first two electrons does not violate the exclusion principle, because the electrons have opposite spins.

4. Therefore, the ground term is  $^3H$ .

#### EXERCISE 11-5

Determine the ground terms for high-spin and low-spin  $d^6$  configurations in  $O_h$  symmetry.

With this review of atomic states, we may now consider the electronic states of coordination compounds and how transitions between these states can give rise to the observed spectra. Before considering specific examples of spectra, however, we must also consider which types of transitions are most probable and, therefore, give rise to the most intense absorptions.

## 11-3-1 SELECTION RULES

The relative intensities of absorption bands are governed by a series of selection rules. On the basis of the symmetry and spin multiplicity of ground and excited electronic states, two of these rules may be stated as follows:<sup>8,9</sup>

1. Transitions between states of the same parity (symmetry with respect to a center of inversion) are forbidden. For example, transitions between  $d$  orbitals are forbidden ( $g \longrightarrow g$  transitions;  $d$  orbitals are symmetric to inversion), but between  $d$  and  $p$  orbitals are allowed ( $g \longrightarrow u$  transitions;  $p$  orbitals are antisymmetric to inversion). This is known as the **Laporte selection rule**.
2. Transitions between states of different spin multiplicities are forbidden. For example, transitions between  $^4A_2$  and  $^4T_1$  states are "spin-allowed," but between  $^4A_2$  and  $^2A_2$  are "spin-forbidden." This is called the **spin selection rule**.

These rules would seem to rule out most electronic transitions for transition metal complexes. However, many such complexes are vividly colored, a consequence of various mechanisms by which these rules can be relaxed. Some of the most important of these mechanisms are as follows:

1. The bonds in transition metal complexes are not rigid but undergo vibrations that may temporarily change the symmetry. Octahedral complexes, for example, vibrate in ways in which the center of symmetry is temporarily lost; this phenomenon, called vibronic coupling, provides a way to relax the first selection rule. As a consequence,  $d-d$  transitions having molar absorptivities in the range of approximately  $10$  to  $50 \text{ L mol}^{-1} \text{ cm}^{-1}$  commonly occur (and are often responsible for the bright colors of many of these complexes).
2. Tetrahedral complexes often absorb more strongly than octahedral complexes of the same metal in the same oxidation state. Metal-ligand sigma bonding in transition metal complexes of  $T_d$  symmetry can be described as involving a combination of  $sp^3$  and  $sd^3$  hybridization of the metal orbitals; both types of hybridization are consistent with the symmetry. The mixing of  $p$ -orbital character (of  $u$  symmetry) with  $d$ -orbital character provides a second way of relaxing the first selection rule.
3. Spin-orbit coupling in some cases provides a mechanism of relaxing the second selection rule, with the result that transitions may be observed from a ground state of one spin multiplicity to an excited state of different spin multiplicity. Such absorption bands for first-row transition metal complexes are usually very weak, with typical molar absorptivities less than  $1 \text{ L mol}^{-1} \text{ cm}^{-1}$ . For complexes of second- and third-row transition metals, spin-orbit coupling can be more important.

Examples of spectra illustrating the selection rules and the ways in which they may be relaxed are given in the following sections of this chapter. Our first example will be a metal complex having a  $d^2$  configuration and octahedral geometry,  $[\text{V}(\text{H}_2\text{O})_6]^{3+}$ .

In discussing spectra, it will be particularly useful to be able to relate the electronic spectra of transition metal complexes to the ligand field splitting,  $\Delta_o$  for octahedral complexes. To do this it will be necessary to introduce two special types of diagrams, **correlation diagrams** and **Tanabe-Sugano diagrams**.

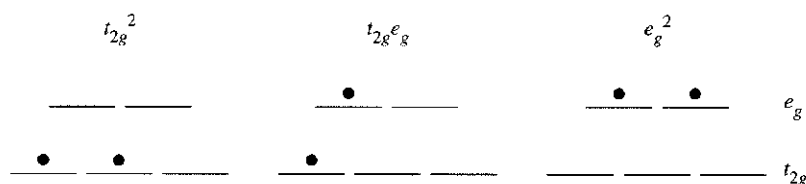
<sup>8</sup>B. N. Figgis and M. A. Hitchman, *Ligand Field Theory and its Applications*, Wiley-VCH, New York, 2000, pp. 181-183.

<sup>9</sup>B. N. Figgis, "Ligand Field Theory", in G. Wilkinson, R. D. Gillard, and J. A. McCleverty, eds., *Comprehensive Coordination Chemistry*, Vol. 1, Pergamon Press, Elmsford, NY, 1987, pp. 243-246.

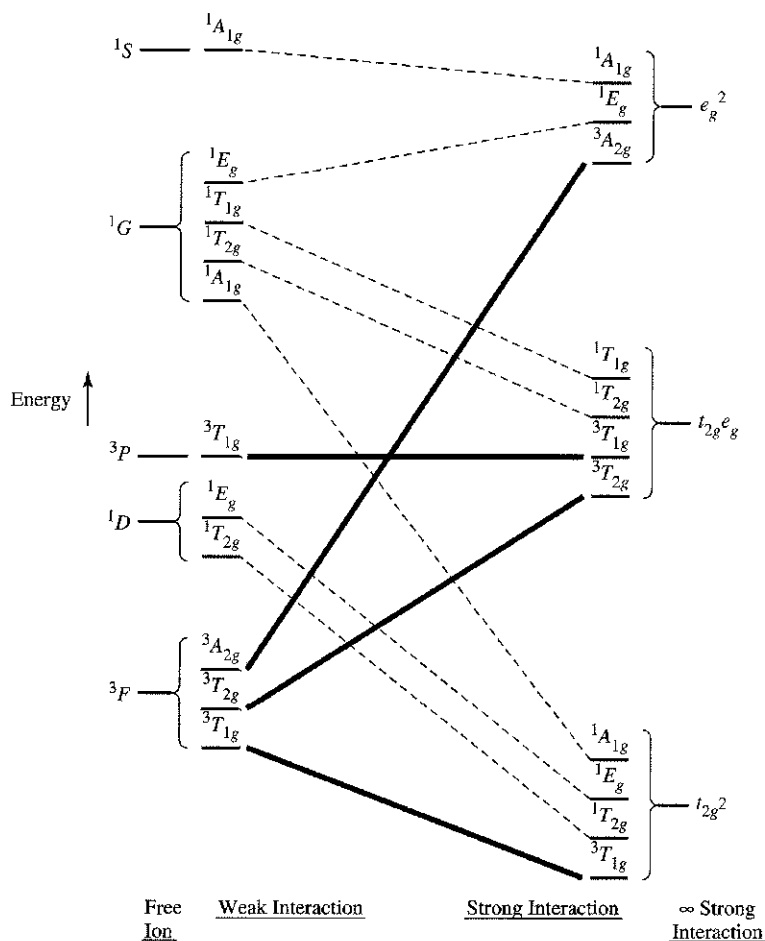
## 11-3-2 CORRELATION DIAGRAMS

Figure 11-3 is an example of a correlation diagram for the configuration  $d^2$ . These diagrams make use of two extremes:

1. **Free ions (no ligand field).** In Exercise 11-4, the terms  ${}^3F$ ,  ${}^3P$ ,  ${}^1G$ ,  ${}^1D$ , and  ${}^1S$  were obtained for a  $d^2$  configuration, with the  ${}^3F$  term having the lowest energy. These terms describe the energy levels of a "free"  $d^2$  ion (in our example, a  $V^{3+}$  ion) in the absence of any interactions with ligands. In correlation diagrams, we will show these free-ion terms on the far left.
2. **Strong ligand field.** There are three possible configurations for two  $d$  electrons in an octahedral ligand field:



In our example, these would be the possible electron configurations of  $V^{3+}$  in an extremely strong ligand field ( $t_{2g}^2$  would be the ground state; the others would be excited states). In correlation diagrams, we will show these states on the far right, as the "strong field limit." Here, the effect of the ligands is so strong that it completely overrides the effects of  $LS$  coupling.



**FIGURE 11-3** Correlation Diagram for  $d^2$  in Octahedral Ligand Field.

In actual coordination compounds, the situation is intermediate between these extremes. At zero field, the  $m_l$  and  $m_s$  values of the individual electrons couple to form, for  $d^2$ , the five terms  ${}^3F$ ,  ${}^3P$ ,  ${}^1G$ ,  ${}^1D$ , and  ${}^1S$ , representing five atomic states with different energies. At a very high ligand field, the  $t_{2g}^2$ ,  $t_{2g}e_g$ , and  $e_g^2$  configurations predominate. The correlation diagram shows the full range of in-between cases in which both factors are important.

Some details of the method for achieving this are beyond the scope of this text; the interested reader should consult the literature<sup>10</sup> for details omitted here. The aspect of this problem that is important to us is that free-ion terms (shown on the far left in the correlation diagrams) have symmetry characteristics that enable them to be reduced to their constituent irreducible representations (in our example, these will be irreducible representations in the  $O_h$  point group). In an octahedral ligand field, the free-ion terms will be split into states corresponding to the irreducible representations, as shown in Table 11-6.

**TABLE 11-6**  
Splitting of Free-ion Terms in Octahedral Symmetry

Term	Irreducible Representations
<i>S</i>	$A_{1g}$
<i>P</i>	$T_{1g}$
<i>D</i>	$E_g + T_{2g}$
<i>F</i>	$A_{2g} + T_{1g} + T_{2g}$
<i>G</i>	$A_{1g} + E_g + T_{1g} + T_{2g}$
<i>H</i>	$E_g + 2T_{1g} + T_{2g}$
<i>I</i>	$A_{1g} + A_{2g} + E_g + T_{1g} + 2T_{2g}$

NOTE: Although representations based on atomic orbitals may have either *g* or *u* symmetry, the terms given here are for *d* orbitals and as a result have only *g* symmetry. See F. A. Cotton, *Chemical Applications of Group Theory*, 3rd ed., Wiley-Interscience, New York, 1990, pp. 263–264, for a discussion of these labels.

Similarly, irreducible representations may be obtained for the strong-field limit configurations (in our example,  $t_{2g}^2$ ,  $t_{2g}e_g$ , and  $e_g^2$ ). The irreducible representations for the two limiting situations must match; each irreducible representation for the free ion must match, or correlate with, a representation for the strong-field limit. This is shown in the correlation diagram for  $d^2$  in Figure 11-3.

Note especially the following characteristics of this correlation diagram:

1. The free-ion states (terms arising from *LS* coupling) are shown on the far left.
2. The extremely strong-field states are shown on the far right.
3. Both the free-ion and strong-field states can be reduced to irreducible representations, as shown. Each free-ion irreducible representation is matched with (correlates with) a strong-field irreducible representation having the same symmetry (same label). As mentioned in Section 11-3-1, transitions to excited states having the same spin multiplicity as the ground state are more likely than transitions to states of different spin multiplicity. To emphasize this, the ground state and states of the same spin multiplicity as the ground state are shown as heavy lines, and states having other spin multiplicities are shown as dashed lines.

In the correlation diagram the states are shown in order of energy. A noncrossing rule is observed: lines connecting states of the same symmetry designation do not cross. Correlation diagrams are available for other *d*-electron configurations.<sup>11</sup>

<sup>10</sup>F. A. Cotton, *Chemical Applications of Group Theory*, 3rd ed., Wiley-Interscience, New York, 1990, Chapter 9, pp. 253–303.

<sup>11</sup>B. N. Figgis and M. A. Hitchman, *Ligand Field Theory and Its Applications*, Wiley-VCH, New York, 2000, pp. 128–134.

## 11-3-3 TANABE-SUGANO DIAGRAMS

Tanabe-Sugano diagrams are special correlation diagrams that are particularly useful in the interpretation of electronic spectra of coordination compounds.<sup>12</sup> In Tanabe-Sugano diagrams, the lowest-energy state is plotted along the horizontal axis; consequently, the vertical distance above this axis is a measure of the energy of the excited state above the ground state. For example, for the  $d^2$  configuration, the lowest-energy state is described by the line in the correlation diagram (Figure 11-3) joining the  ${}^3T_{1g}$  state arising from the  ${}^3F$  free-ion term with the  ${}^3T_{1g}$  state arising from the strong-field term,  $t_{2g}^2$ . In the Tanabe-Sugano diagram (Figure 11-4), this line is made horizontal; it is labeled  ${}^3T_{1g}(F)$  and is shown to arise from the  ${}^3F$  term in the free-ion limit (left side of diagram).<sup>13</sup>

The Tanabe-Sugano diagram also shows excited states. In the  $d^2$  diagram, the excited states of the same spin multiplicity as the ground state are the  ${}^3T_{2g}$ ,  ${}^3T_{1g}(P)$ , and the  ${}^3A_{2g}$ . The reader should verify that these are the same triplet excited states shown in the  $d^2$  correlation diagram. Excited states of other spin multiplicities are also shown but, as we will see, they are generally not as important in the interpretation of spectra.

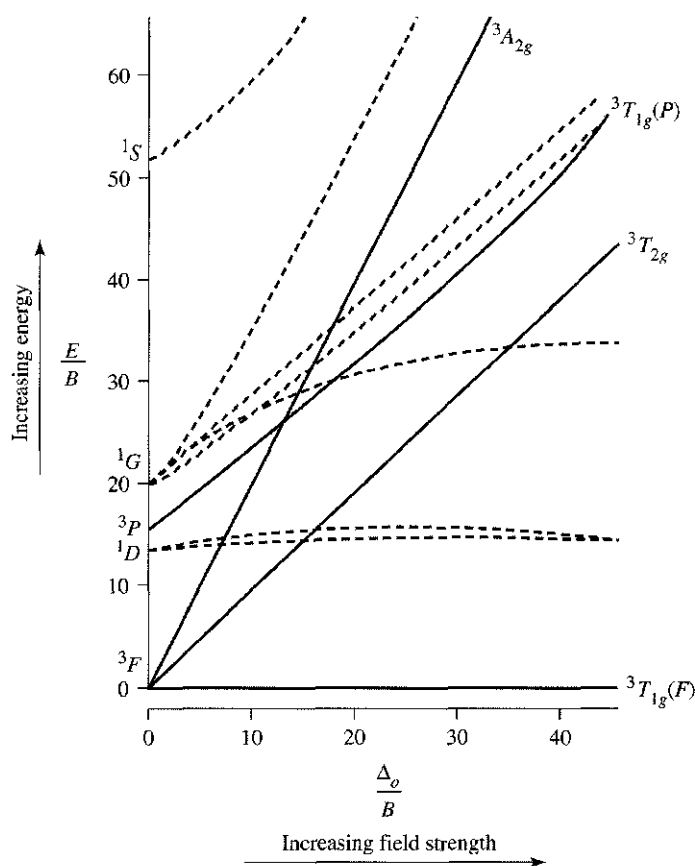


FIGURE 11-4 Tanabe-Sugano Diagram for  $d^2$  in Octahedral Ligand Field.

<sup>12</sup>Y. Tanabe and S. Sugano, *J. Phys. Soc. Japan*, 1954, 9, 766.

<sup>13</sup>The  $F$  in parentheses distinguishes this  ${}^3T_{1g}$  term from the higher energy  ${}^3T_{1g}$  term arising from the  ${}^3P$  term in the free-ion limit.

The quantities plotted in a Tanabe-Sugano diagram are as follows:

Horizontal axis:  $\frac{\Delta_o}{B}$  where  $\Delta_o$  is the octahedral ligand field splitting, described in Chapter 10.

$B =$  Racah parameter, a measure of the repulsion between terms of the same multiplicity. For  $d^2$ , for example, the energy difference between  ${}^3F$  and  ${}^3P$  is  $15B$ .<sup>14</sup>

Vertical axis:  $\frac{E}{B}$  where  $E$  is the energy (of excited states) above the ground state.

As mentioned, one of the most useful characteristics of Tanabe-Sugano diagrams is that *the ground electronic state is always plotted along the horizontal axis*; this makes it easy to determine values of  $E/B$  above the ground state.

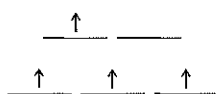
### EXAMPLE

**$[\text{V}(\text{H}_2\text{O})_6]^{3+}$  ( $d^2$ )** A good example of the utility of Tanabe-Sugano diagrams in explaining electronic spectra is provided by the  $d^2$  complex  $[\text{V}(\text{H}_2\text{O})_6]^{3+}$ . The ground state is  ${}^3T_{1g}(F)$ ; under ordinary conditions this is the only electronic state that is appreciably occupied. Absorption of light should occur primarily to excited states also having a spin multiplicity of 3. There are three of these,  ${}^3T_{2g}$ ,  ${}^3T_{1g}(P)$ , and  ${}^3A_{2g}$ . Therefore, three allowed transitions are expected, as shown in Figure 11-5. Consequently, we expect three absorption bands for  $[\text{V}(\text{H}_2\text{O})_6]^{3+}$ , one corresponding to each allowed transition. Is this actually observed for  $[\text{V}(\text{H}_2\text{O})_6]^{3+}$ ? Two bands are readily observed at  $17,800$  and  $25,700 \text{ cm}^{-1}$ , as can be seen in Figure 11-6.<sup>15</sup> A third band, at approximately  $38,000 \text{ cm}^{-1}$ , is apparently obscured in aqueous solution by charge transfer bands nearby (charge transfer bands of coordination compounds will be discussed later in this chapter). In the solid state, however, a band attributed to the  ${}^3T_{1g} \rightarrow {}^3A_{2g}$  transition is observed at  $38,000 \text{ cm}^{-1}$ . These bands match the transitions  $\nu_1$ ,  $\nu_2$ , and  $\nu_3$  indicated on the Tanabe-Sugano diagram (Figure 11-5).

### Other electron configurations

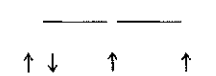
Tanabe-Sugano diagrams for  $d^2$  through  $d^8$  are shown in Figure 11-7. The cases of  $d^1$  and  $d^9$  configurations will be discussed in Section 11-3-4. The diagrams for  $d^4$ ,  $d^5$ ,  $d^6$ , and  $d^7$  have apparent discontinuities, marked by vertical lines near the center. These are configurations for which low spin and high spin are both possible. For example, consider the configuration  $d^4$ :

High-spin (weak-field)  $d^4$  has four unpaired electrons, of parallel spin; such a configuration has a spin multiplicity of 5.



$$S = 4\left(\frac{1}{2}\right) = 2; \quad \text{spin multiplicity} = 2S + 1 = 2(2) + 1 = 5$$

Low-spin (strong-field)  $d^4$ , on the other hand, has only two unpaired electrons and a spin multiplicity of 3.



$$S = 2\left(\frac{1}{2}\right) = 1; \quad \text{spin multiplicity} = 2S + 1 = 2(1) + 1 = 3$$

<sup>14</sup>For a discussion of Racah parameters, see Figgis, "Ligand Field Theory," in *Comprehensive Coordination Chemistry*, Vol. 1, p. 232.

<sup>15</sup>The third band is in the ultraviolet and is off-scale to the right in the spectrum shown; see B. N. Figgis, *Introduction to Ligand Fields*, Wiley-Interscience, New York, 1966, p. 219.



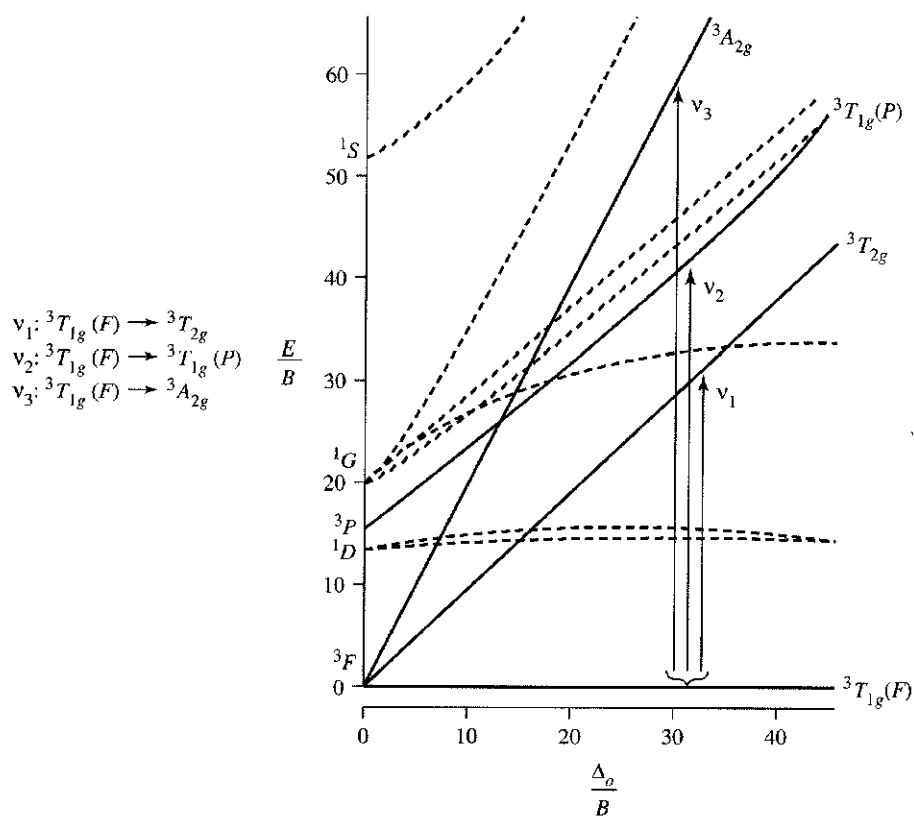


FIGURE 11-5 Spin-allowed Transitions for  $d^2$  Configuration.

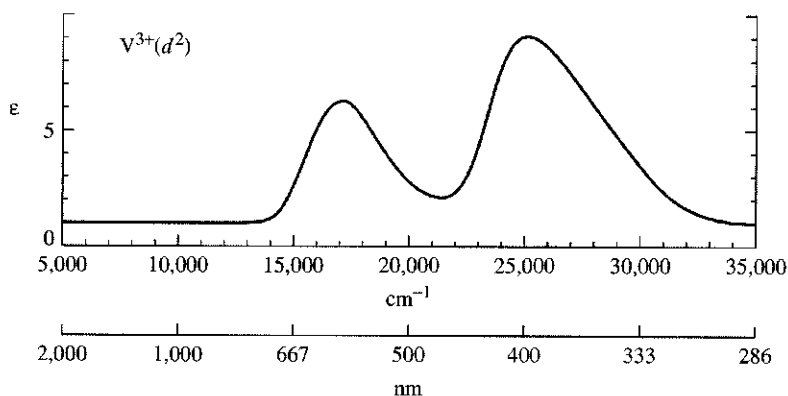
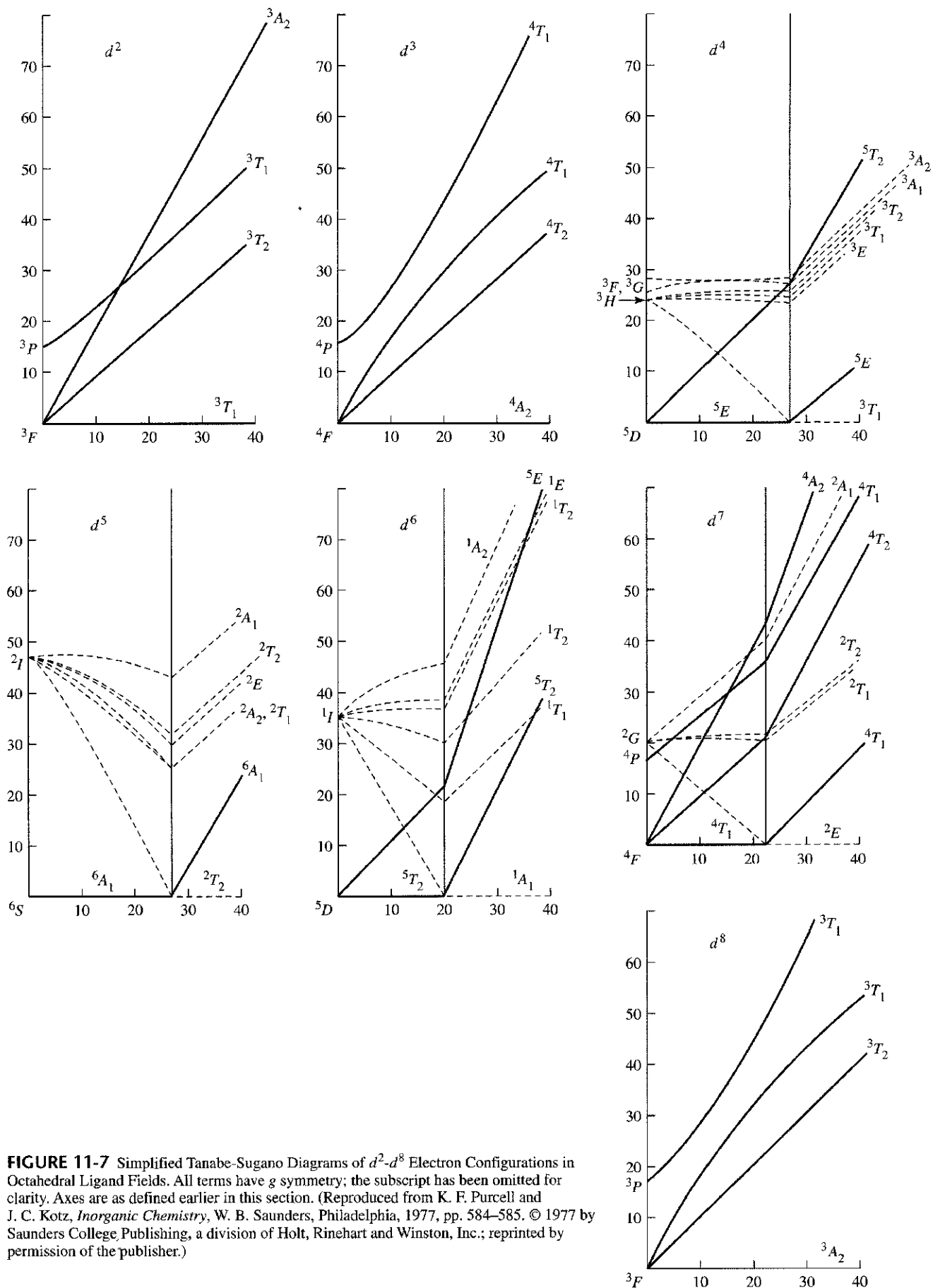


FIGURE 11-6 Absorption Spectrum of  $[\text{V}(\text{H}_2\text{O})_6]^{3+}$ . (Reproduced with permission from B. N. Figgis, *Introduction to Ligand Fields*, Wiley-Interscience, New York, 1966, p. 221.)

In the weak-field part of the Tanabe-Sugano diagram (left of  $\Delta_o/B = 27$ ), the ground state is  ${}^5E_g$ , having the expected spin multiplicity of 5. On the right (strong-field) side of the diagram, the ground state is  ${}^3T_{1g}$  (correlating with the  ${}^3H$  term in the free-ion limit), having the required spin multiplicity of 3. The vertical line is thus a dividing line between weak- and strong-field cases: high-spin (weak-field) complexes are to the left of this line and low-spin (strong-field) complexes are to the right. At the dividing line, the ground state changes from  ${}^5E_g$  to  ${}^3T_{1g}$ . The spin multiplicity changes from 5 to 3 to reflect the change in the number of unpaired electrons.



**FIGURE 11-7** Simplified Tanabe-Sugano Diagrams of  $d^2$ - $d^8$  Electron Configurations in Octahedral Ligand Fields. All terms have g symmetry; the subscript has been omitted for clarity. Axes are as defined earlier in this section. (Reproduced from K. F. Purcell and J. C. Kotz, *Inorganic Chemistry*, W. B. Saunders, Philadelphia, 1977, pp. 584-585. © 1977 by Saunders College Publishing, a division of Holt, Rinehart and Winston, Inc.; reprinted by permission of the publisher.)

Figure 11-8 shows absorption spectra of first-row transition metal complexes of the formula  $[M(H_2O)_6]^{n+}$ . Because water is a rather weak-field ligand, these are all high-spin complexes, represented by the left side of the Tanabe-Sugano diagrams. It is an interesting exercise to compare the number of bands in these spectra with the number of bands expected from the respective Tanabe-Sugano diagrams. Note that in some cases absorption bands are off-scale, farther into the ultraviolet than the spectral region shown.

In Figure 11-8, molar absorptivities (extinction coefficients) are shown on the vertical scale. The absorptivities for most bands are similar (1 to 20  $L mol^{-1} cm^{-1}$ ) except for the spectrum of  $[Mn(H_2O)_6]^{2+}$ , which has much weaker bands. Solutions of  $[Mn(H_2O)_6]^{2+}$  are an extremely pale pink, much more weakly colored than solutions of the other ions shown. Why is absorption by  $[Mn(H_2O)_6]^{2+}$  so weak? To answer this question, it is useful to examine the corresponding Tanabe-Sugano diagram, in this case for a  $d^5$  configuration. We expect  $[Mn(H_2O)_6]^{2+}$  to be a high-spin complex, because  $H_2O$  is a rather weak-field ligand. The ground state for

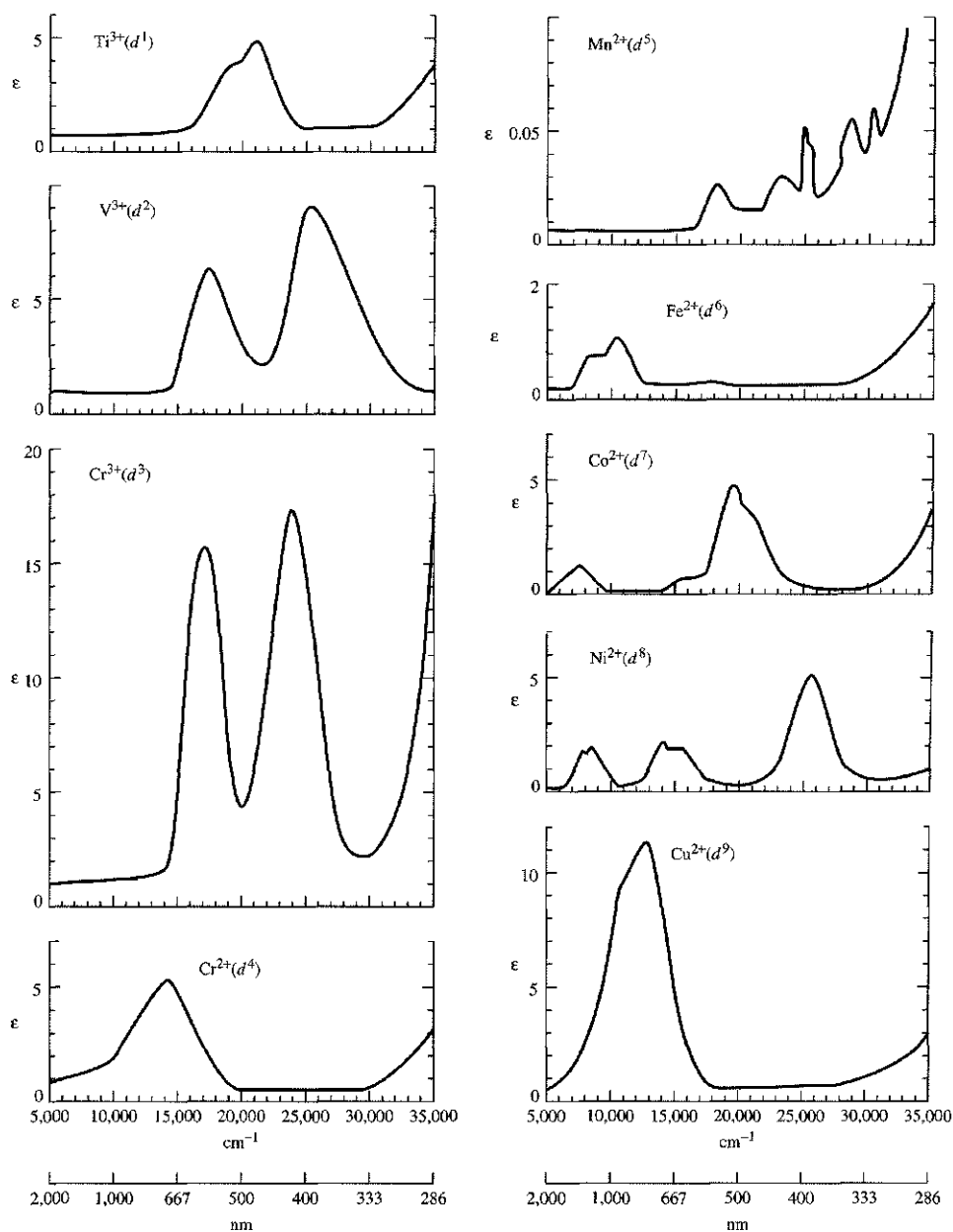
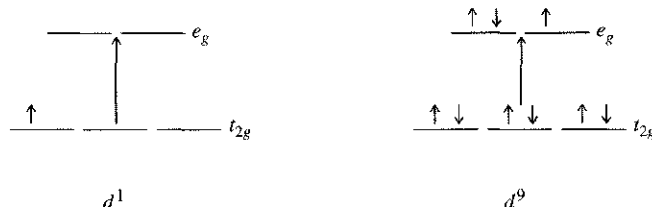


**FIGURE 11-8** Electronic Spectra of First-Row Transition Metal Complexes of Formula  $[M(H_2O)_6]^{n+}$ . (Reproduced with permission from B. N. Figgis, *Introduction to Ligand Fields*, Wiley-Interscience, New York, 1966, pp. 221, 224.)

weak-field  $d^5$  is the  ${}^6A_{1g}$ . There are no excited states of the same spin multiplicity (6), and consequently there can be no spin-allowed absorptions. That  $[\text{Mn}(\text{H}_2\text{O})_6]^{2+}$  is colored at all is a consequence of very weak forbidden transitions to excited states of spin multiplicity other than 6 (there are many such excited states, hence the rather complicated spectrum).

### 11-3-4 JAHN-TELLER DISTORTIONS AND SPECTRA

Up to this point, we have not discussed the spectra of  $d^1$  and  $d^9$  complexes. By virtue of the simple  $d$ -electron configurations for these cases, we might expect each to exhibit one absorption band corresponding to excitation of an electron from the  $t_{2g}$  to the  $e_g$  levels:



However, this view must be at least a modest oversimplification, because examination of the spectra of  $[\text{Ti}(\text{H}_2\text{O})_6]^{3+}$  ( $d^1$ ) and  $[\text{Cu}(\text{H}_2\text{O})_6]^{2+}$  ( $d^9$ ) (see Figure 11-8) shows these coordination compounds to exhibit two closely overlapping absorption bands rather than a single band.

To account for the apparent splitting of bands in these examples, it is necessary to recall that, as described in Section 10-5, some configurations can cause complexes to be distorted. In 1937, Jahn and Teller showed that nonlinear molecules having a degenerate electronic state should distort to lower the symmetry of the molecule and to reduce the degeneracy; this is commonly called the Jahn-Teller theorem.<sup>16</sup> For example, a  $d^9$  metal in an octahedral complex has the electron configuration  $t_{2g}^6 e_g^3$ ; according to the Jahn-Teller theorem, such a complex should distort. If the distortion takes the form of an elongation along the  $z$  axis (the most common distortion observed experimentally), the  $t_{2g}$  and  $e_g$  orbitals are affected as shown in Figure 11-9. Distortion from  $O_h$  to  $D_{4h}$  symmetry results in stabilization of the molecule: the  $e_g$  orbital is split into a lower  $a_{1g}$  level and a higher  $b_{1g}$  level.

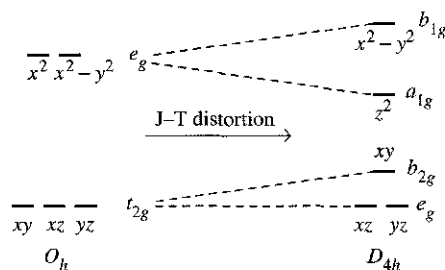
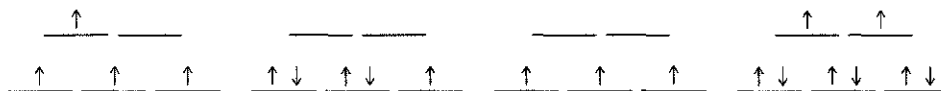


FIGURE 11-9 Effect of Jahn-Teller Distortion on  $d$  Orbitals of Octahedral Complex.

When degenerate orbitals are asymmetrically occupied, Jahn-Teller distortions are likely. For example, the first two configurations below should give distortions, but the third and fourth should not:



<sup>16</sup>B. Bersucker, *Coord. Chem. Rev.*, **1975**, *14*, 357.

In practice, the only electron configurations for  $O_h$  symmetry that give rise to measurable Jahn-Teller distortions are those that have asymmetrically occupied  $e_g$  orbitals, such as the high-spin  $d^4$  configuration. The Jahn-Teller theorem does not predict what the distortion will be; by far, the most common distortion observed is elongation along the  $z$  axis. Although the Jahn-Teller theorem predicts that configurations having asymmetrically occupied  $t_{2g}$  orbitals, such as the low-spin  $d^5$  configuration, should also be distorted, such distortions are too small to be measured in most cases.

The Jahn-Teller effect on spectra can easily be seen from the example of  $[\text{Cu}(\text{H}_2\text{O})_6]^{2+}$ , a  $d^9$  complex. From Figure 11-9, which shows the effect on  $d$  orbitals of distortion from  $O_h$  to  $D_{4h}$  geometry, we can see the additional splitting of orbitals accompanying the reduction of symmetry.

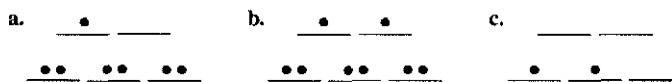
### Symmetry labels for configurations

Electron configurations have symmetry labels that match their degeneracies, as follows:

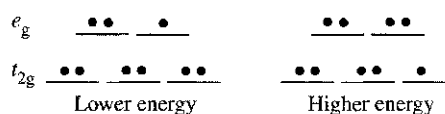
		<i>Examples</i>	
$T$	designates a triply degenerate asymmetrically occupied state.		
$E$	designates a doubly degenerate asymmetrically occupied state.		
$A$ or $B$	designate a nondegenerate state. Each set of levels in an $A$ or $B$ state is symmetrically occupied.		

#### EXERCISE 11-6

Identify the following configurations as  $T$ ,  $A$ , or  $E$  states in octahedral complexes:



When a  ${}^2D$  term for  $d^9$  is split by an octahedral ligand field, two configurations result:



The lower energy configuration is doubly degenerate in the  $e_g$  orbitals (occupation of the  $e_g$  orbitals could be  $\bullet\bullet$  or  $\bullet\bullet$ ) and has the designation  ${}^2E_g$ ; the higher energy configuration is triply degenerate in the  $t_{2g}$  levels (three arrangements are possible in these levels:  $\bullet\bullet$ ,  $\bullet\bullet$ , or  $\bullet\bullet$ ) and has the designation  ${}^2T_{2g}$ . Thus, the lower energy configuration is the  ${}^2E_g$ , and the higher energy configuration is the  ${}^2T_{2g}$ , as in Figure 11-10. This is the opposite of the order of energies of the orbitals ( $t_{2g}$  lower than  $e_g$ ), shown in Figure 11-9.

Similarly, for distortion to  $D_{4h}$ , the order of labels of the orbitals in Figure 11-9 is the reverse of the order of labels of the energy configurations in Figure 11-10.

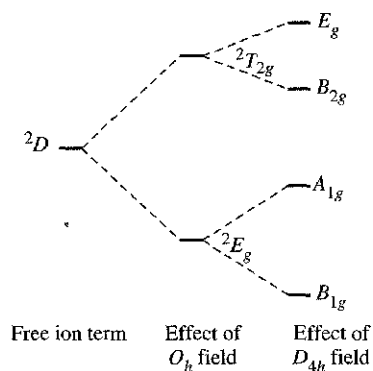
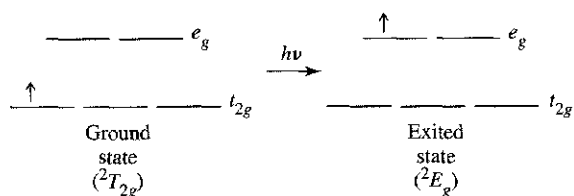


**FIGURE 11-10** Splitting of Octahedral Free-ion Terms on Jahn-Teller Distortion for  $d^9$  Configuration.

In summary, the  ${}^2D$  free-ion term is split into  ${}^2E_g$  and  ${}^2T_{2g}$  by a field of  $O_h$  symmetry, and further split on distortion to  $D_{4h}$  symmetry. The labels of the states resulting from the free-ion term (Figure 11-10) are in reverse order to the labels on the orbitals; for example, the  $b_{1g}$  atomic orbital is of highest energy, whereas the  $B_{1g}$  state originating from the  ${}^2D$  free-ion term is of lowest energy.<sup>17</sup>

For a  $d^9$  configuration, the ground state in octahedral symmetry is a  ${}^2E_g$  term and the excited state is a  ${}^2T_{2g}$  term. On distortion to  $D_{4h}$  geometry, these terms split, as shown in Figure 11-10. In an octahedral  $d^9$  complex, we would expect excitation from the  ${}^2E_g$  state to the  ${}^2T_{2g}$  state and a single absorption band. Distortion of the complex to  $D_{4h}$  geometry splits the  ${}^2T_{2g}$  level into two levels, the  $E_g$  and the  $B_{2g}$ . Excitation can now occur from the ground state (now the  $B_{1g}$  state) to the  $A_{1g}$ , the  $E_g$ , or the  $B_{2g}$  (the splitting is exaggerated in Figure 11-10). The  $B_{1g} \rightarrow A_{1g}$  transition is too low in energy to be observed in the visible spectrum. If the distortion is strong enough, therefore, two separate absorption bands may be observed in the visible region, to the  $E_g$  or the  $B_{2g}$  levels (or a broadened or narrowly split peak is found, as in  $[\text{Cu}(\text{H}_2\text{O})_6]^{2+}$ ).

For a  $d^1$  complex, a single absorption band, corresponding to excitation of a  $t_{2g}$  electron to an  $e_g$  orbital, might be expected:



However, the spectrum of  $[\text{Ti}(\text{H}_2\text{O})_6]^{3+}$ , an example of a  $d^1$  complex, shows two apparently overlapping bands rather than a single band. How is this possible?

One explanation commonly used is that the excited state can undergo Jahn-Teller distortion,<sup>18</sup> as in Figure 11-10. As in the examples considered previously, asymmetric occupation of the  $e_g$  orbitals can split these orbitals into two of slightly different energy (of  $A_{1g}$  and  $B_{1g}$  symmetry). Excitation can now occur from the  $t_{2g}$  level to either of these orbitals. Therefore, as in the case of the  $d^9$  configuration, there are now two excited states of slightly different energy. The consequence may be a broadening of a

<sup>17</sup>Figgis, "Ligand Field Theory," in *Comprehensive Coordination Chemistry*, Vol. 1, pp. 252-253.

<sup>18</sup>C. J. Ballhausen, *Introduction to Ligand Field Theory*, McGraw-Hill, New York, 1962, p. 227, and references therein.

spectrum into a two-humped peak, as in  $[\text{Ti}(\text{H}_2\text{O})_6]^{3+}$ , or in some cases into two more clearly defined separate peaks.<sup>19</sup>

One additional point needs to be made in regard to Tanabe-Sugano diagrams. These diagrams, as shown in Figure 11-8, assume  $O_h$  symmetry, in excited states as well as ground states. The consequence is that the diagrams are useful in predicting the general properties of spectra; in fact, many complexes do have sharply defined bands that fit the Tanabe-Sugano description well (see the  $d^2$ ,  $d^3$ , and  $d^4$  examples in Figure 11-8). However, distortions from pure octahedral symmetry are rather common, and the consequence can be the splitting of bands—or, in some cases of severe distortion, situations in which the bands are difficult to interpret. Additional examples of spectra showing the splitting of absorption bands can be seen in Figure 11-8.

#### EXERCISE 11-7

$[\text{Fe}(\text{H}_2\text{O})_6]^{2+}$  has a two-humped absorption peak near 1000 nm. By using the appropriate Tanabe-Sugano diagram, account for the most likely origin of this absorption. Then, account for the splitting of the absorption band.

### 11-3-5 EXAMPLES OF APPLICATIONS OF TANABE-SUGANO DIAGRAMS: DETERMINING $\Delta_o$ FROM SPECTRA

Absorption spectra of coordination compounds can be used to determine the magnitude of the ligand field splitting, which is  $\Delta_o$  for octahedral complexes. It should be made clear from the outset that the accuracy with which  $\Delta_o$  can be determined is to some extent limited by the mathematical tools used to solve the problem. Absorption spectra often have overlapping bands; to determine the positions of the bands accurately, therefore, requires an appropriate mathematical technique for reducing overlapping bands into their individual components. Such analysis is beyond the scope of this text. However, we can often obtain  $\Delta_o$  values (and sometimes values of the Racah parameter,  $B$ ) of reasonable accuracy simply by using the positions of the absorption maxima taken directly from the spectra.

The ease with which  $\Delta_o$  can be determined depends on the  $d$ -electron configuration of the metal; in some cases,  $\Delta_o$  can be read easily from a spectrum, but in other cases a more complicated analysis is necessary. The following discussion will proceed from the simplest cases to the most complicated.

#### $d^1$ , $d^4$ (high spin), $d^6$ (high spin), $d^9$

Each of these cases, as shown in Figure 11-11, corresponds to a simple excitation of an electron from a  $t_{2g}$  to an  $e_g$  orbital, with the final (excited) electron configuration having the same spin multiplicity as the initial configuration. In each case, there is a single excited state of the same spin multiplicity as the ground state. Consequently, there is a single spin-allowed absorption, with the energy of the absorbed light equal to  $\Delta_o$ . Examples of such complexes include  $[\text{Ti}(\text{H}_2\text{O})_6]^{3+}$ ,  $[\text{Cr}(\text{H}_2\text{O})_6]^{2+}$ ,  $[\text{Fe}(\text{H}_2\text{O})_6]^{2+}$ , and  $[\text{Cu}(\text{H}_2\text{O})_6]^{2+}$ ; note from Figure 11-8 that each of these complexes exhibits essentially a single absorption band. In some cases, splitting of bands due to Jahn-Teller distortion is observed, as discussed in Section 11-3-4.

<sup>19</sup>F. A. Cotton and G. Wilkinson, *Advanced Inorganic Chemistry*, 4th ed., Wiley-Interscience, New York, 1980, pp. 680–681.

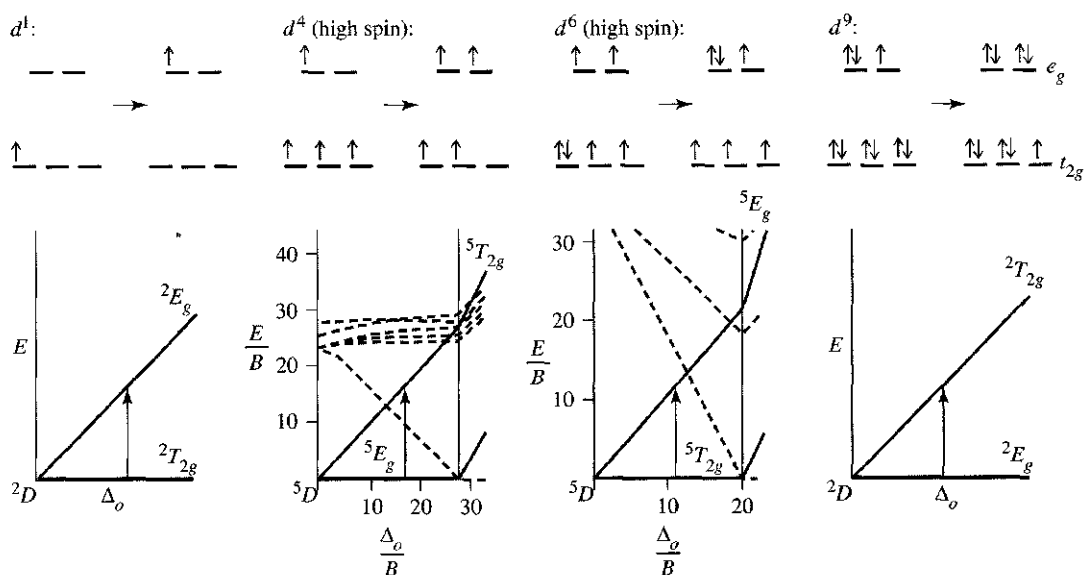


FIGURE 11-11 Determining  $\Delta_o$  for  $d^1$ ,  $d^4$  (High Spin),  $d^6$  (High Spin), and  $d^9$  Configurations.

### $d^3$ , $d^8$

These electron configurations have a ground state  $F$  term. In an octahedral ligand field, an  $F$  term splits into three terms, an  $A_{2g}$ , a  $T_{2g}$ , and a  $T_{1g}$ . As shown in Figure 11-12, the  $A_{2g}$  is of lowest energy for  $d^3$  or  $d^8$ . For these configurations, the difference in energy between the two lowest-energy terms, the  $A_{2g}$  and the  $T_{2g}$ , is equal to  $\Delta_o$ . Therefore, to find  $\Delta_o$ , we simply find the energy of the lowest-energy transition in the absorption spectrum. Examples include  $[\text{Cr}(\text{H}_2\text{O})_6]^{3+}$  and  $[\text{Ni}(\text{H}_2\text{O})_6]^{2+}$ . In each case, the lowest-energy band in the spectra of these complexes (Figure 11-8) is for the transition from the  ${}^4A_{2g}$  ground state to the  ${}^4T_{2g}$  excited state. The energies of these bands, approximately 17,500 and 8,500  $\text{cm}^{-1}$ , respectively, are the corresponding values of  $\Delta_o$ .

### $d^2$ , $d^7$ (high spin)

As in the case of  $d^3$  and  $d^8$ , the ground free-ion terms for these two configurations are  $F$  terms. However, the determination of  $\Delta_o$  is not as simple for  $d^2$  and  $d^7$ . To explain this, it is necessary to take a close look at the Tanabe-Sugano diagrams. We will compare the  $d^3$  and  $d^2$  Tanabe-Sugano diagrams; the  $d^8$  and  $d^7$  (high-spin) cases can be compared in a similar fashion [note the similarity of the  $d^3$  and  $d^8$  Tanabe-Sugano diagrams and of the  $d^2$  and  $d^7$  (high-spin region) diagrams].

In the  $d^3$  case, the ground state is a  ${}^4A_{2g}$  state. There are three excited quartet states,  ${}^4T_{2g}$ ,  ${}^4T_{1g}$  (from  ${}^4F$  term), and  ${}^4T_{1g}$  (from  ${}^4P$  term). Note the two states of the same symmetry ( ${}^4T_{1g}$ ). An important property of such states is that states of the same symmetry may mix. The consequence of such mixing is that, as the ligand field is increased, the states appear to repel each other; the lines in the Tanabe-Sugano diagram curve away from each other. This effect can easily be seen in the Tanabe-Sugano diagram for  $d^3$  (see Figure 11-7). However, this causes no difficulty in obtaining  $\Delta_o$  for a



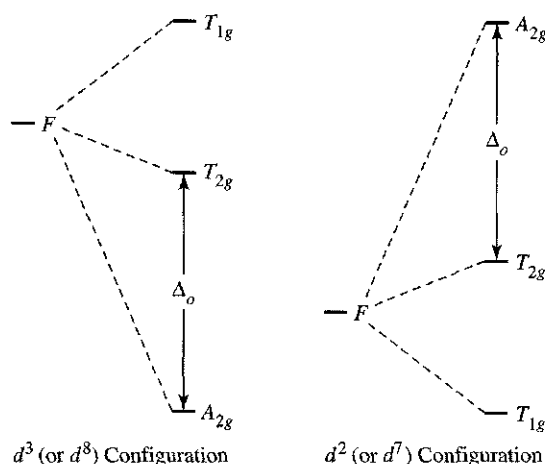


FIGURE 11-12 Splitting of  $F$  Terms in Octahedral Symmetry.

$d^3$  complex, because the lowest-energy transition ( ${}^4A_{2g} \longrightarrow {}^4T_{2g}$ ) is not affected by such curvature. (The Tanabe-Sugano diagram shows that the energy of the  ${}^4T_{2g}$  state varies linearly with the strength of the ligand field.)

The situation in the  $d^2$  case is not quite as simple. For  $d^2$ , the free-ion  ${}^3F$  term is also split into  ${}^3T_{1g} + {}^3T_{2g} + {}^3A_{2g}$ ; these are the same states obtained from  $d^3$ , but in reverse order (Figure 11-12). For  $d^2$ , the ground state is  ${}^3T_{1g}$ . It is tempting to simply determine the energy of the  ${}^3T_{1g}(F) \longrightarrow {}^3T_{2g}$  band and assign this as the value of  $\Delta_o$ . After all, the  ${}^3T_{1g}(F)$  can be identified with the configuration  $t_{2g}^2$  (see correlation diagram, Figure 11-3), and  ${}^3T_{2g}$  with the configuration  $t_{2g}e_g$ ; the difference between these states should give  $\Delta_o$ . However, the  ${}^3T_{1g}(F)$  state can mix with the  ${}^3T_{1g}$  state arising from the  ${}^3P$  free-ion term, causing a slight curvature of both in the Tanabe-Sugano diagram. This curvature can lead to some error in using the ground state to obtain values of  $\Delta_o$ .

Therefore, we must resort to an alternative: to determine the difference in energy between the  $t_{2g}e_g$  and  $e_g^2$  configurations, which should also be equal to  $\Delta_o$  (because the energy necessary to excite a single electron from a  $t_{2g}$  to an  $e_g$  orbital is equal to  $\Delta_o$ ). This means that we can use the difference between  ${}^3T_{2g}$  (for the  $t_{2g}e_g$  configuration) and  ${}^3A_{2g}$  (for  $e_g^2$ ; see Figure 11-3) to calculate  $\Delta_o$ :

$$\begin{aligned} & \text{energy of transition } {}^3T_{1g} \longrightarrow {}^3A_{2g} \\ & - \text{energy of transition } {}^3T_{1g} \longrightarrow {}^3T_{2g} \\ \hline \Delta_o = & \text{energy difference between } {}^3A_{2g} \text{ and } {}^3T_{2g} \end{aligned} \quad (\text{see Figure 11-13})$$

The difficulty with this approach is that two lines cross in the Tanabe-Sugano diagram. Therefore, the assignment of the absorption bands may be in question. From the diagram for  $d^2$ , we can see that although the lowest energy absorption band (to  ${}^3T_{2g}$ ) is easily assigned, there are two possibilities for the next band: to  ${}^3A_{2g}$  for very weak field ligands, or to  ${}^3T_{1g}(P)$  for stronger field ligands. In addition, the second and third absorption bands may overlap, making it difficult to determine the exact positions of the bands (the apparent positions of absorption maxima may be shifted if the bands overlap). In such cases a more complicated analysis, involving a calculation of the Racah parameter,  $B$ , may be necessary. This procedure is best illustrated by the following example.

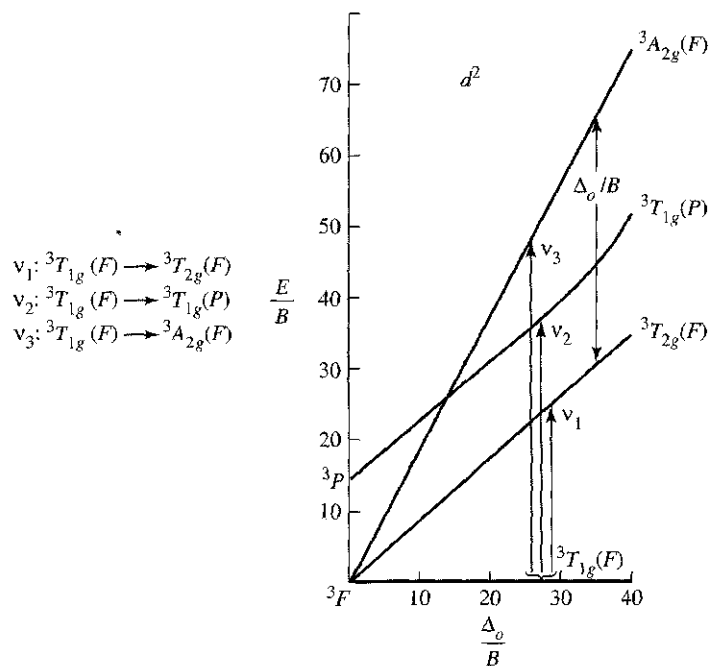
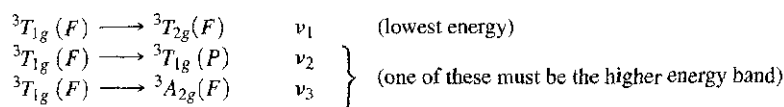


FIGURE 11-13 Spin-allowed Transitions for  $d^2$  Configuration.

#### EXAMPLE

$[\text{V}(\text{H}_2\text{O})_6]^{3+}$  has absorption bands at  $17,800$  and  $25,700 \text{ cm}^{-1}$ . Using the Tanabe-Sugano diagram for  $d^2$ , estimate values of  $\Delta_o$  and  $B$  for this complex.

From the Tanabe-Sugano diagram there are three possible spin-allowed transitions (Figure 11-13):



When working with spectra, it is often useful to determine the ratio of energies of the absorption bands. In this example,

$$\frac{25,700 \text{ cm}^{-1}}{17,800 \text{ cm}^{-1}} = 1.44$$

The ratio of energy of the higher energy transition ( $\nu_2$  or  $\nu_3$ ) to the lowest-energy transition ( $\nu_1$ ) must therefore be approximately 1.44. From the Tanabe-Sugano diagram, we can see that the ratio of  $\nu_3$  to  $\nu_1$  is approximately 2, regardless of the strength of the ligand field; we can therefore eliminate  $\nu_3$  as the possible transition occurring at  $25,700 \text{ cm}^{-1}$ . This means that the  $25,700 \text{ cm}^{-1}$  band must be  $\nu_2$ , corresponding to  ${}^3T_{1g}(F) \longrightarrow {}^3T_{1g}(P)$ , and

$$1.44 = \frac{\nu_2}{\nu_1}$$

The ratio  $\nu_2/\nu_1$  varies as a function of the strength of the ligand field. By plotting the ratio  $\nu_2/\nu_1$  versus  $\Delta_o/B$  (Figure 11-14), we find that  $\nu_2/\nu_1 = 1.44$  at approximately  $\Delta_o/B = 31$ .<sup>20,21</sup>

<sup>20</sup>N. N. Greenwood and A. Earnshaw, *Chemistry of the Elements*, Pergamon Press, Elmsford, NY, 1984, p. 1161; B. N. Figgis and M. A. Hitchman, *Ligand Field Theory and Its Applications*, Wiley-VCH, New York, 2000, pp. 189–193.

<sup>21</sup>Different references report slightly different positions for the absorption bands of  $[\text{V}(\text{H}_2\text{O})_6]^{3+}$  and hence slightly different values of  $B$  and  $\Delta_o$ .

$\Delta_o/B$	$E/B$		$\nu_2/\nu_1$
	$\nu_1$	$\nu_2$	
0	0	15	—
10	8.74	21.5	2.46
20	18.2	31.4	1.73
30	27.9	40.8	1.46
40	37.7	50.4	1.34
50	47.6	60.2	1.26

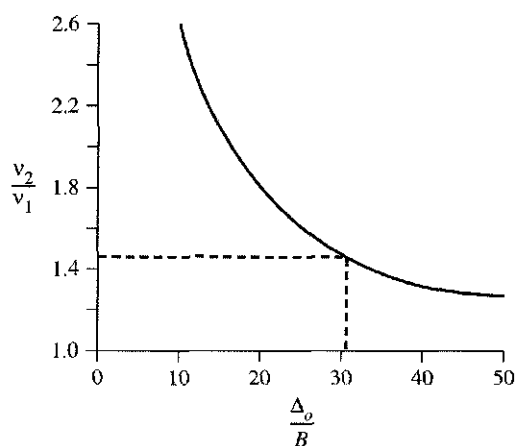


FIGURE 11-14 Value of  $\nu_1/\nu_2$  Ratio for  $d^2$  Configuration.

At  $\frac{\Delta_o}{B} = 31$ :

$$\nu_2: \frac{E}{B} = 42 \text{ (approximately); } B = \frac{E}{42} = \frac{25,700 \text{ cm}^{-1}}{42} = 610 \text{ cm}^{-1}$$

$$\nu_1: \frac{E}{B} = 29 \text{ (approximately); } B = \frac{E}{29} = \frac{17,800 \text{ cm}^{-1}}{29} = 610 \text{ cm}^{-1}$$

Because  $\frac{\Delta_o}{B} = 31$ :

$$\Delta_o = 31 \times B = 31 \times 610 \text{ cm}^{-1} = 19,000 \text{ cm}^{-1}$$

This procedure can be followed for  $d^2$  and  $d^7$  complexes of octahedral geometry to estimate values for  $\Delta_o$  (and  $B$ ).

#### EXERCISE 11-8

Use the Co(II) spectrum in Figure 11-8 and the Tanabe-Sugano diagrams of Figure 11-7 to find  $\Delta_o$  and  $B$ . The broad band near  $20,000 \text{ cm}^{-1}$  can be considered to have the  ${}^4T_{1g} \longrightarrow {}^4A_{2g}$  transition in the small shoulder near  $16,000 \text{ cm}^{-1}$  and the  ${}^4T_{1g}(F) \longrightarrow {}^4T_{1g}(P)$  transition at the peak.<sup>22</sup>

### Other configurations: $d^5$ (high spin), $d^4$ to $d^7$ (low spin)

As has been mentioned previously, high-spin  $d^5$  complexes have no excited states of the same spin multiplicity (6) as the ground state. The bands that are observed are therefore the consequence of spin-forbidden transitions and are typically very weak as, for example, in  $[\text{Mn}(\text{H}_2\text{O})_6]^{2+}$ . The interested reader is referred to the literature<sup>23</sup> for an analysis of such spectra. In the case of low-spin  $d^4$  to  $d^7$  octahedral complexes, the analysis can be difficult, since there are many excited states of the same spin multiplicity as the ground state (see right side of Tanabe-Sugano diagrams for  $d^4$  to  $d^7$ , Figure 11-7). Again, the chemical literature provides examples and analyses of the spectra of such compounds.<sup>24</sup>

<sup>22</sup>The  ${}^4T_{1g} \longrightarrow {}^4A_{2g}$  transition is generally weak in octahedral complexes of  $\text{Co}^{2+}$ , because such a transition corresponds to simultaneous excitation of two electrons and is less probable than the other spin-allowed transitions, which are for excitations of single electrons.

<sup>23</sup>B. N. Figgis and M. A. Hitchman, *Ligand Field Theory and Its Applications*, Wiley-VCH, New York, 2000, pp. 208–209.

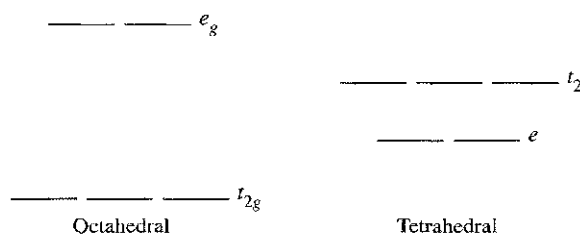
<sup>24</sup>Figgis and Hitchman, *Ligand Field Theory and its Applications*, pp. 204–207; B. N. Figgis, in G. Wilkinson, R. D. Gillard, and J. A. McCleverty, eds., *Comprehensive Coordination Chemistry*, Vol. 1, Pergamon, Elmsford, NY, 1987, pp. 243–246.

## 11-3-6 TETRAHEDRAL COMPLEXES

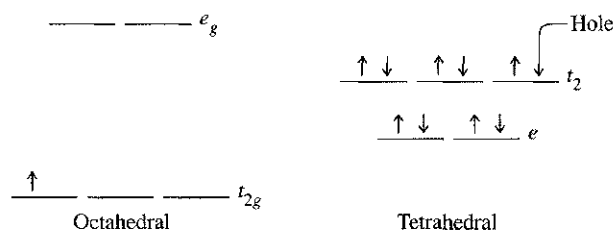
In general, tetrahedral complexes have more intense absorptions than octahedral complexes. This is a consequence of the first (Laporte) selection rule (Section 11-3-1): transitions between  $d$  orbitals in a complex having a center of symmetry are forbidden. As a result, absorption bands for octahedral complexes are weak (small molar absorptivities); that they absorb at all is the result of vibrational motions that act continually to distort molecules slightly from pure  $O_h$  symmetry.

In tetrahedral complexes, the situation is different. The lack of a center of symmetry makes transitions between  $d$  orbitals more allowed; the consequence is that tetrahedral complexes often have much more intense absorption bands than octahedral complexes.<sup>25</sup>

As we have seen, the  $d$  orbitals for tetrahedral complexes are split in the opposite fashion to octahedral complexes:



A useful comparison can be drawn between these by using what is called the **hole formalism**. This can best be illustrated by example. Consider a  $d^1$  configuration in an octahedral complex. The one electron occupies an orbital in a triply degenerate set ( $t_{2g}$ ). Now, consider a  $d^9$  configuration in a tetrahedral complex. This configuration has a “hole” in a triply degenerate set of orbitals ( $t_2$ ). It can be shown that, in terms of symmetry, the  $d^1 O_h$  configuration is analogous to the  $d^9 T_d$  configuration; the “hole” in  $d^9$  results in the same symmetry as the single electron in  $d^1$ .



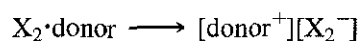
In practical terms, this means that, for tetrahedral geometry, we can use the correlation diagram for the  $d^{10-n}$  configuration in octahedral geometry to describe the  $d^n$  configuration in tetrahedral geometry. Thus, for a  $d^2$  tetrahedral case, we can use the  $d^8$  octahedral correlation diagram, for the  $d^3$  tetrahedral case we can use the  $d^7$  octahedral diagram, and so on. We can then identify the appropriate spin-allowed bands as in octahedral geometry, with allowed transitions occurring between the ground state and excited states of the same spin multiplicity.

<sup>25</sup>Two types of hybrid orbitals are possible for a central atom of  $T_d$  symmetry:  $sd^3$  and  $sp^3$  (see Chapter 5). These types of hybrids may be viewed as mixing, to yield hybrid orbitals that contain some  $p$  character (note that  $p$  orbitals are not symmetric to inversion), as well as  $d$  character. The mixing in of  $p$  character can be viewed as making transitions between these orbitals more allowed. For a more thorough discussion of this phenomenon, see F. A. Cotton, *Chemical Applications of Group Theory*, 3rd ed., Wiley-Interscience, New York, 1990, pp. 295–296. Pages 289–297 of this reference also give a more detailed discussion of other selection rules.

Other geometries can also be considered according to the same principles as for octahedral and tetrahedral complexes. The interested reader is referred to the literature for a discussion of different geometries.<sup>26</sup>

### 11-3-7 CHARGE-TRANSFER SPECTRA

Examples of charge-transfer absorptions in solutions of halogens have been described in Chapter 6. In these cases, a strong interaction between a donor solvent and a halogen molecule,  $X_2$ , leads to the formation of a complex in which an excited state (primarily of  $X_2$  character) can accept electrons from a HOMO (primarily of solvent character) on absorption of light of suitable energy:



The absorption band, known as a **charge-transfer band**, can be very intense; it is responsible for the vivid colors of some of the halogens in donor solvents.

It is extremely common for coordination compounds also to exhibit strong charge-transfer absorptions, typically in the ultraviolet and/or visible portions of the spectrum. These absorptions may be much more intense than *d-d* transitions (which for octahedral complexes usually have  $\epsilon$  values of  $20 \text{ L mol}^{-1} \text{ cm}^{-1}$  or less); molar absorptivities of  $50,000 \text{ L mole}^{-1} \text{ cm}^{-1}$  or greater are not uncommon for these bands. Such absorption bands involve the transfer of electrons from molecular orbitals that are primarily ligand in character to orbitals that are primarily metal in character (or vice versa). For example, consider an octahedral  $d^6$  complex with  $\sigma$ -donor ligands. The ligand electron pairs are stabilized, as shown in Figure 11-15.

The possibility exists that electrons can be excited, not only from the  $t_{2g}$  level to the  $e_g$  but also from the  $\sigma$  orbitals originating from the ligands to the  $e_g$ . The latter excitation results in a charge-transfer transition; it may be designated as **charge transfer to metal (CTTM)** or **ligand to metal charge transfer (LMCT)**. This type of transition results in formal reduction of the metal. A CTTM excitation involving a cobalt (III) complex, for example, would exhibit an excited state having cobalt(II).

Examples of charge-transfer absorptions are numerous. For example, the octahedral complexes  $\text{IrBr}_6^{2-}$  ( $d^5$ ) and  $\text{IrBr}_6^{3-}$  ( $d^6$ ) both show charge-transfer bands. For  $\text{IrBr}_6^{2-}$ , two bands appear, near 600 nm and near 270 nm; the former is attributed to transitions to the  $t_{2g}$  levels and the latter to the  $e_g$ . In  $\text{IrBr}_6^{3-}$ , the  $t_{2g}$  levels are filled, and the only possible CTTM absorption is therefore to the  $e_g$ . Consequently, no low-energy absorptions in the 600-nm range are observed, but strong absorption is seen near

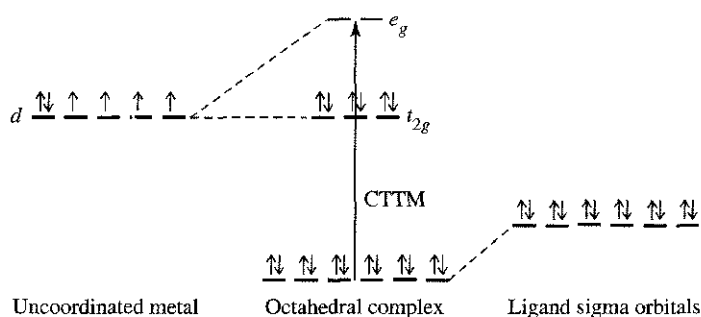


FIGURE 11-15 Charge Transfer to Metal.

<sup>26</sup>Figgis and Hitchman, *Ligand Field Theory and Its Applications*, pp. 211–214; Cotton, *Chemical Applications of Group Theory*, 3rd ed., pp. 295–303.

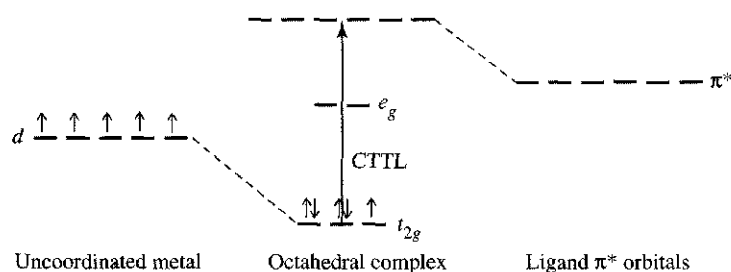


FIGURE 11-16 Charge Transfer to Ligand.

250 nm, corresponding to charge transfer to  $e_g$ . A common example of tetrahedral geometry is the permanganate ion,  $\text{MnO}_4^-$ , which is intensely purple because of a strong absorption involving charge transfer from orbitals derived primarily from the filled oxygen  $p$  orbitals to empty orbitals derived primarily from the manganese(VII).

Similarly, it is possible for there to be **charge transfer to ligand (CTTL)**, also known as **metal to ligand charge transfer (MLCT)**, transitions in coordination compounds having  $\pi$ -acceptor ligands. In these cases, empty  $\pi^*$  orbitals on the ligands become the acceptor orbitals on absorption of light. Figure 11-16 illustrates this phenomenon for a  $d^5$  complex.

CTTL results in oxidation of the metal; a CTTL excitation of an iron(III) complex would give an iron(IV) excited state. CTTL most commonly occurs with ligands having empty  $\pi^*$  orbitals, such as  $\text{CO}$ ,  $\text{CN}^-$ ,  $\text{SCN}^-$ , bipyridine, and dithiocarbamate ( $\text{S}_2\text{CNR}_2^-$ ).

In complexes such as  $\text{Cr}(\text{CO})_6$  which have both  $\sigma$ -donor and  $\pi$ -acceptor orbitals, both types of charge transfer are possible. It is not always easy to determine the type of charge transfer in a given coordination compound. Many ligands give highly colored complexes that have a series of overlapping absorption bands in the ultraviolet part of the spectrum as well as the visible. In such cases, the  $d-d$  transitions may be completely overwhelmed and essentially impossible to observe.

Finally, the ligand itself may have a chromophore and still another type of absorption band, an **intraligand band**, may be observed. These bands may sometimes be identified by comparing the spectra of complexes with the spectra of free ligands. However, coordination of a ligand to a metal may significantly alter the energies of the ligand orbitals, and such comparisons may be difficult, especially if charge-transfer bands overlap the intraligand bands. Also, it should be noted that not all ligands exist in the free state; some ligands owe their existence to the ability of metal atoms to stabilize molecules that are otherwise highly unstable. Examples of several such ligands will be discussed in later chapters.

#### EXERCISE 11-9

The isoelectronic ions  $\text{VO}_4^{3-}$ ,  $\text{CrO}_4^{2-}$ , and  $\text{MnO}_4^-$  all have intense charge transfer transitions. The wavelengths of these transitions increase in this series, with  $\text{MnO}_4^-$  having its charge-transfer absorption at the longest wavelength. Suggest a reason for this trend.

#### GENERAL REFERENCES

B. N. Figgis and M. A. Hitchman, *Ligand Field Theory and Its Applications*, Wiley-VCH, New York, 2000, and B. N. Figgis, "Ligand Field Theory," in G. Wilkinson, R. D. Gillard, and J. A. McCleverty, eds., *Comprehensive Coordination Chemistry*, Vol. 1, Pergamon Press, Elmsford, NY, 1987, pp. 213–280, provide extensive background in the theory of electronic spectra, with numerous examples. Also useful is C. J. Ballhausen, *Introduction to Ligand Field Theory*, McGraw-Hill, New York, 1962. Important aspects of symmetry applied to this topic can be found in F. A. Cotton, *Chemical Applications of Group Theory*, 3rd ed., Wiley-Interscience, New York, 1990.

## PROBLEMS

- 11-1** For each of the following configurations, construct a microstate table and reduce the table to its constituent free-ion terms. Identify the lowest-energy term for each.
- $p^3$
  - $p^1 d^1$  (as in a  $4p^1 3d^1$  configuration)
- 11-2** For each of the lowest-energy (ground state) terms in Problem 11-1, determine the possible values of  $J$ . Which  $J$  value describes the state with the lowest energy?
- 11-3** For each of the following free-ion terms, determine the values of  $L$ ,  $M_L$ ,  $S$ , and  $M_S$ :
- ${}^2D (d^3)$
  - ${}^3G (d^4)$
  - ${}^4F (d^7)$
- 11-4** For each of the free-ion terms in Problem 11-3, determine the possible values of  $J$ , and decide which is the lowest in energy.
- 11-5** The most intense absorption band in the visible spectrum of  $[\text{Mn}(\text{H}_2\text{O})_6]^{2+}$  is at  $24,900 \text{ cm}^{-1}$  and has a molar absorptivity of  $0.038 \text{ L mol}^{-1} \text{ cm}^{-1}$ . What concentration of  $[\text{Mn}(\text{H}_2\text{O})_6]^{2+}$  would be necessary to give an absorbance of 0.10 in a cell of path length 1.00 cm?
- 11-6**
- Determine the wavelength and frequency of  $24,900 \text{ cm}^{-1}$  light.
  - Determine the energy and frequency of 366 nm light.
- 11-7** Determine the ground terms for the following configurations:
- $d^8$  ( $O_h$  symmetry)
  - High-spin and low-spin  $d^5$  ( $O_h$  symmetry)
  - $d^4$  ( $T_d$  symmetry)
  - $d^9$  ( $D_{4h}$  symmetry, square-planar)
- 11-8** The spectrum of  $[\text{Ni}(\text{H}_2\text{O})_6]^{2+}$  (Figure 11-8) shows three principal absorption bands, with two of the bands showing signs of further splitting. Referring to the Tanabe-Sugano diagram, estimate the value of  $\Delta_o$ . Give a likely explanation for the further splitting of the spectrum.
- 11-9** From the following spectral data, and using Tanabe-Sugano diagrams (Figure 11-7), calculate  $\Delta_o$  for the following:
- $[\text{Cr}(\text{C}_2\text{O}_4)_3]^{3-}$ , which has absorption bands at  $23,600$  and  $17,400 \text{ cm}^{-1}$ . A third band occurs well into the ultraviolet.
  - $[\text{Ti}(\text{NCS})_6]^{3-}$ , which has an asymmetric, slightly split band at  $18,400 \text{ cm}^{-1}$ . (Also, suggest a reason for the splitting of this band.)
  - $[\text{Ni}(\text{en})_3]^{2+}$ , which has three absorption bands:  $11,200$ ,  $18,350$ , and  $29,000 \text{ cm}^{-1}$ .
  - $[\text{VF}_6]^{3-}$ , which has two absorption bands at  $14,800$  and  $23,250 \text{ cm}^{-1}$ , plus a third band in the ultraviolet. (Also, calculate  $B$  for this ion.)
  - The complex  $\text{VCl}_3(\text{CH}_3\text{CN})_3$ , which has absorption bands at 694 and 467 nm. Calculate  $\Delta_o$  and  $B$  for this complex.
- 11-10**  $[\text{Co}(\text{NH}_3)_6]^{2+}$  has absorption bands at  $9,000$  and  $21,100 \text{ cm}^{-1}$ . Calculate  $\Delta_o$  and  $B$  for this ion. (Hints: The  ${}^4T_{1g} \rightarrow {}^4A_{2g}$  transition in this complex is too weak to be observed. The graph in Figure 11-13 may be used for  $d^7$  as well as  $d^2$  complexes.)
- 11-11** Classify the following configurations as  $A$ ,  $E$ , or  $T$  in complexes having  $O_h$  symmetry. Some of these configurations represent excited states.
- $t_{2g}^4 e_g^2$
  - $t_{2g}^6$
  - $t_{2g}^3 e_g^3$
  - $t_{2g}^5$
  - $e_g$
- 11-12** Of the first-row transition metal complexes of formula  $[\text{M}(\text{NH}_3)_6]^{3+}$ , which metals are predicted by the Jahn-Teller theorem to have distorted complexes?
- 11-13**  $\text{MnO}_4^-$  is a stronger oxidizing agent than  $\text{ReO}_4^-$ . Both ions have charge-transfer bands; however, the charge-transfer band for  $\text{ReO}_4^-$  is in the ultraviolet, whereas the corresponding band for  $\text{MnO}_4^-$  is responsible for its intensely purple color. Are the relative positions of the charge transfer absorptions consistent with the oxidizing abilities of these ions? Explain.